Journal of Cleaner Production 275 (2020) 124112

Contents lists available at ScienceDirect

Journal of Cleaner Production

journal homepage: www.elsevier.com/locate/jclepro

A relative robust optimization for a vehicle routing problem with time-window and synchronized visits considering greenhouse gas emissions

Yong Shi [a, b], Yanjie Zhou [c, d, *], Wenhui Ye [e], Qian Qian Zhao [c, d]

[a] UMR SADAPT, INRAE, AgroParisTech, Université Paris-Saclay, Rue de Claude Bertand, 75005, Paris, France
[b] Nanomedicine Lab, Université Bourgogne Franche-Comté, UTBM, Rue Ernest Thierry Mieg, 90010, Belfort, France
[c] School of Management Engineering, Zhengzhou University, 450001, Zhengzhou, China
[d] Department of Industrial Engineering, Pusan National University, 46421, Busan, Republic of Korea
[e] Business Incubation Base, China University of Geosciences, 430074, Wuhan, China

ARTICLE INFO

Article history:
Received 18 May 2020
Received in revised form
30 August 2020
Accepted 4 September 2020
Available online 12 September 2020

Handling Editor: M.T. Moreira

Keywords:
Synchronized visits
Relative robust optimization
Greenhouse gas emissions
Time window
Vehicle routing problem

ABSTRACT

The Paris Agreement appeals to all countries around the world for reducing greenhouse gas emissions. Nowadays, logistics companies do not only consider improving service quality and reducing operating costs but also should take a particular corporate social responsibility: reducing greenhouse gas emissions. Minimizing greenhouse gas emissions has been emerged in vehicle routing problems in many investigations, while most of the models are deterministic. The feedback from logistics practice reveals that the workers often encounter uncertainties when providing services to customers. The decisions made without considering uncertainties show less robustness when carrying the logistics activities according to the given scheduling. Consequently, in this study, this is the first attempt to develop a relative robust optimization model for a vehicle routing problem with synchronized visits and uncertain scenarios considering greenhouse gas emissions. In this study the greenhouse gas emissions is evaluated by the fuel consumption cost. Due to the NP-hard of the studied model, a hybrid tabu search and simulated annealing is proposed to solve it. The experimental results on the popularly used benchmark instances demonstrate that the proposed algorithm is efficient and effective. The comparison performed among the solutions obtained by different types of models has highlighted the importance of considering uncertainties. Then, the sensitivity analysis is performed to observe the change of fuel consumption cost with varying types of vehicles. Statistical analysis is carried out to further validate the different models. Finally, two bi-objective optimization based scenarios have been established to demonstrate the trade-off between GHG emissions and robustness indicators. The proposed models can be applied to some practical applications, such as logging truck routing planing.

1. Introduction

Recently, global warming has been involved by scientists, governments, social society and public. Environmentalists appeal us to pay more attention to the environmental issues (Ding et al., 2020) and take immediate actions to safeguard our homes and futures on this planet. The greenhouse gas (GHG) emissions, which are generated by human activities, are the most significant cause of observed climate changes. As shown in Fig. 1, statistical results indicate that the transport sector in the USA ranks the first position in terms of greenhouse gas emissions in 2017. As part of an effort to reduce GHG emissions, the European Union set a goal of reducing transport-related emissions by 60% in 2050 from 1990 levels. In 2015, the United States of America, which was one of the biggest polluters in the world, accounted for 15% of global carbon emissions from fuel combustion (UCS, 2019). According to a news reported by CNN in 2019, the United Kingdom aims to be the first country in the G7 economy with net-zero carbon emissions by 2050 (Westcott

* Corresponding author. Department of Industrial Engineering, Pusan National University, 46421, Busan, Republic of Korea.
E-mail addresses: shiyonghbwh@gmail.com (Y. Shi), y.j.zhou.g@gmail.com (Y. Zhou).

https://doi.org/10.1016/j.jclepro.2020.124112
0959-6526/

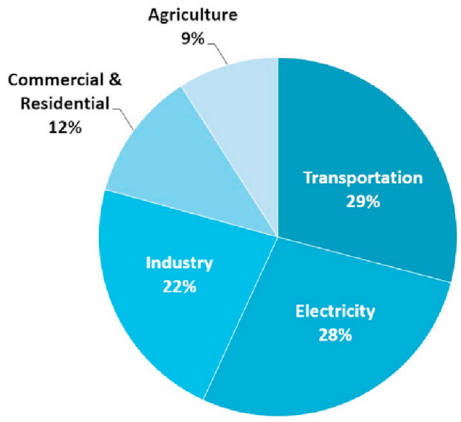

Fig. 1. The greenhouse gas[1]emissions by sector in the US, (Hockstad and Hanel).

and Wilkinson, 2019). The United Kingdom government is taking all the possible actions to cut carbon emissions.

Nowadays, logistics companies, as profit-making enterprises, do not only consider improving service quality and reducing operating costs but also should take a certain corporate social responsibility for reducing greenhouse gas emissions. From the perspective of operational management, the main procedures of services in logistics companies can be roughly divided into three steps (Shi et al., 2017). First, a logistics company will be involved in collecting information from its customers. The customers provide their basic information such as the customers' condition, demanded service types. After gathering all the information from customers, the company plans or reschedules a scheme to arrange the workers, demands, and devices to visit the customers. Operational research and other data science approach are usually employed to help the decision-makers to make a good schedule, which can arrange the limited resources (labor resources and equipment) efficiently utilized. After that, each worker drives a car to visit the customers' home one by one according to the scheduling given by the logistics company.

In addition to greenhouse gas emissions, improving logistics operation efficiency has also been a major concern of logistics companies. The practice has shown that workers encountered a lot of uncertainties. Travel time is affected by weather, road conditions, traffic jams, and other factors. Besides that service time can be affected by, for example, the customer's actual condition and the difficulty of finding a parking space. For example, the home health care service is a time-sensitive service (Shi et al., 2018b). At 11:00 a.m., an old adult with diabetes needs to inject insulin on time. At that time, serious delays may lead to serious affect on the health of the elderly. It can be seen that a reasonable and stable schedule not only helps to reduce operating costs but also helps to improve customer satisfaction and attracts more customers.

Recently, vehicle synchronization constraints have attracted the attention of researchers. This constraint is primarily described as the need for two workers to drive different vehicles, reach the customer's home, and provide services to the customer simultaneously. According to the definition of synchronization constraints, once a worker is delayed, another worker cannot provide the entire service, so the entire service must face a waiting state until all the workers arrive. This puts higher demands on stable travel and service hours. Table 1 reveals the arrival and waiting situation of workers. The table shows that the customers waiting for the workers account for five kinds of scenarios in the whole nine scenarios. However, workers are allowed to wait but not customers during the services. The workers' waiting can be regarded as a kind of rest. However, a delayed service for a customer may result in uncomfortable and displeasure. Therefore, in VRP with synchronization constraints, robustness is more significance.

Motivated by the aforementioned investigation, in this study, a VRP with time-window and synchronized visits considering greenhouse gas emissions (GVRPTWSyn) is investigated. Due to the reality of VRP scenarios, it always incurs uncertain factors, including traffic jams, the uncertainty of service time, etc. Therefore, the logistics company can make a more reasonable schedule if the uncertainties are considered in advance.

Generally speaking, the uncertainties could be considered into the optimization model either via fuzzy chance-constraint programming (FCCP), stochastic programming (SP) (Fu et al., 2019), or robust optimization (RO) (Hu et al., 2018). In the FCCP, the uncertain variables are assumed to be fuzzy variables, and the credibility theory established by Liu and Zhao (1998) is often utilized to construct the model. SP often assumes a probability distribution (e.g., normal distribution), and the mathematical expectation value of a recourse function is added to the objective function. However, RO assumes that such probability information is unknown. RO generally uses uncertainty sets to characterize uncertainties. Commonly used uncertainty sets include box/ellipsoid uncertainty set, budgeted uncertainty set, and so on. SP generally optimizes expected values, and robust optimization optimizes worst-cast cost/profit scenarios, which can make the obtained optimal solutions perform more robust. In logistics services, it is difficult to give the distribution characteristics of travel time and service time. Even if this distribution law is known in advance, it is difficult to estimate the values of the parameters. To ensure that the company could be obtain a robust solution (RO-GVRPTWSyn[2]), in this article, robust optimization is selected as a modeling tool.

As the VRP itself is an NP-hard problem, and the problem considered in this study is an extension of VRP, with more difficult synchronization constraints in a robust optimization model. There is no doubt that RO-GVRPTWSyn is also an NP-hard problem, which is a computational challenge. According to the relevant work (Liu et al., 2019), heuristic algorithms are usually considered to solve this kind of problem. In this work, a hybrid simulated annealing (SA) and tabu search (TS) is designed. According to our trials, SA usually has strong global searchability while shows less local searchability in the early stage of the algorithm. Meanwhile, TS has good local searchability, as well as an excellent memory-based strategy for getting rid of the local optimal solutions. Therefore, the hybrid SA and TS can boost the performance of the searching ability both globally and locally. Additionally, the proposed algorithm integrates the advantages of SA and TS to guide the searching process to escape from the local minimum. Besides, some new components are also added to the framework of the algorithm with the features of the studied problem. To our best knowledge, our study is the first time for designing hybrid SA and TS for solving VRP with synchronization.

From the perspective of optimization technology, the proposed model is more difficult than the previous studies in two aspects.

- In the deterministic model, the dummy customers are introduced to describe the synchronization service, and this means that when performing the local search operators, they should be

[1] The greenhouse gases is mainly composed by methane, carbon dioxide, water vapor and ozone.

[2] The problem considered in this study is abbreviated as RO-GVRPTWSyn.

Table 1
The different situations of the arrival times of the worker A and B.

B	A			
		early arrival	Arrive on time	Arrive late
	early arrival	A and B: waiting (fine)	B waiting (fine)	B and customer: waiting (bad)
	arrive on time	A: waiting (fine)	no waiting (fine)	B and customer: waiting (bad)
	arrive late	A and customer: waiting (bad)	A and customer: waiting (bad)	A, B and customer: waiting (bad)

ensured to be serviced simultaneously. For example, when performing an intra-route operation on route a1, e.g., 2-opt, the corresponding dummy customer who located route a2 must also be modified. Therefore the starting service time of the other customers on route a2 may also be changed. Consequently, the feasibility of the solution may also be changed. Therefore, the complexity of the algorithm will increase.

- The RO framework is used to formulate our model. RO helps seek the worst cases of the model, which indicates that the RO model minimizes the maximum value of the objective function. Therefore the problem becomes a min_max problem, which is model difficult than the general linear optimization model. Three complicated recursive functions are derived in different scenarios.

The contributions of the our research are summarized as follows.

- Despite that the green VRPs have been widely investigated (Fathollahi-Fard et al., 2018), most of the models are deterministic. This is the first time that green VRP with synchronized visits and uncertain scenarios considering greenhouse gas emissions is studied with the RO perspective. Considering that uncertainties always exist, our model is closer to the reality of life.
- The RO-GVRPTWSyn is computationally challenging due to its NP-hard natural; therefore, an effective hybrid simulated annealing and tabu search algorithm is proposed to solve the robust optimization model. The hybrid algorithm combines the advantages of two heuristic algorithms, making it have good global search and local search capabilities.
- According to the definition of the RO and theory of the budget, the recursive function are derived for getting the largest arrival time of the workers in different scenarios. The comparisons between the results obtained by the deterministic model and the robust optimization models highlight the importance of considering service and travel times simultaneously.
- The change of the amount of greenhouse gas emissions is analyzed with the different scenarios of the robust models. Additionally, the trade-off between GHG emissions and robustness indicators is discussed by performing Pareto-based bi-objective optimization instead of the classical mono-objective optimization framework.

The remainder of this study is presented as follows. Section 2 summarizes the recent work related to the RO-GVRPTWSyn. The deterministic mathematical model and RO model are introduced in Section 3 and 4, respectively. Solution methods are illustrated and analyzed in Section 5. Section 6 reports the experimental results. In the end, conclusions and future studies are discussed.

2. Literature review

As presented above, related literature are divided into the following three categories. The first part is the green VRP, then the applications of synchronized visits constraints and the last one is VRP with uncertainties.

2.1. Green vehicle routing problem

With the widespread concern of environmental protection and sustainability, growing researches related to greenhouse gas emissions (He et al., 2017) are investigated. In recent years, green logistics is more and more popular(Abdi et al., 2019; Zulvia et al., 2020). One of the earliest work was done by Kara et al. (2007) with proposing a liner integer formulation for solving the energy minimization problem in VRP. Kara et al. (2007) found that various factors, including vehicle load, time spent, gasoline price, traveling distance, etc. may affect the travel cost of a given starting node and ending node. As a landmark research, Bektaş and Laporte (2011) proposed a mathematical model named as the pollution routing problem. Bektaş and Laporte (2011) extended the VRP with considering the travel distance, GHG emissions, fuel, traveling time, and other costs in the objective function.

Recently, many mathematical models of green VRP have been established and applied to different industries for logistics transportation. Xiao et al. (2018) designed a new cuckoo search for a patients-transportation-problem considering transport emissions in the healthcare industry. Macrina et al. (2019) studied a mixed green fleet VRP considering the partial battery recharging and time windows in which the mixed fleet includes conventional and electric vehicles. Li et al. (2019) introduced a novel ant colony optimization algorithm to settle a multi-depot green VRP with maximizing revenue and minimizing costs, time, and emission. Zulvia et al. (2020) proposed a many-objective gradient evolution algorithm for a green VRP considering time windows and time dependency for perishable products. One of the important branches of GVRP is electric vehicle routing problem (Montoya et al., 2017). Basso et al. (2019) addressed a two-stage electrical vehicle routing problem with taking into account the energy consumption, which is estimated by the speed of the vehicle and topography. Finally, they indicated that the estimation of the energy consumption is more exact than the state-of-art. Almouhanna et al. (2020) investigated the location-routing problem with the limitation of the travel distance when utilizing electric vehicles. In their study, they consider the location problem and vehicle routing problem simultaneously. As a feature in this transportation system, they added constraints of travel distances to the electric vehicles. Finally, the model is solved with a multi-start heuristic approach.

Green VRP can be viewed as the extension of VRP, which has been proven to be an NP-hard problem. Therefore green VRP is also an NP-hard problem. Consequently, real-world, large-scale instances are difficult to be solved directly with commercial software, such as CPLEX solver and Gurobi Solver. For solving the proposed green VRP models, the researchers developed various algorithms that can be divided into two categories, including exact algorithms and meta-heuristics. Some of the related algorithms are summarized in Table 2.

Table 2
Summary of the algorithms contributed in the green VRP.

Papers	Exact algorithms					Heuristics
	Branch & Cut	Branch & Bound	Branch & Pricing	Column Generation	Bender Decomposition	
Ropke and Pisinger (2006)					✓	
Trautsamwieser et al. (2011)			✓			
Rodriguez et al. (2015)	✓					
En-nahli et al. (2016)						Iterated local search
Shi et al. (2017)						Hybrid genetic algorithm
Alvarez and Munari (2017)	✓		✓			
Munari and Morabito (2018)	✓		✓			
Shi et al. (2018b)						Simulated annealing
Cappanera et al. (2018)						Matheuristic approximation
Shi et al. (2019)						Tabu search
Fathollahi-Fard et al. (2019)						Simulated annealing
Haddadene et al. (2019)						Multi-Start NSGAII
Liu et al. (2019)						Adaptive large neighborhood search
Li et al. (2019)						Ant colony optimization
Zhang et al. (2019)	✓	✓	✓			
Li et al. (2019)				✓		
Faiz et al. (2019)				✓		

2.2. VRP with synchronized visits

In addition to greenhouse gas emissions, synchronization constraint is another interesting point in VRP. The constraint of synchronized visits indicates that two or more workers provide service for a customer simultaneously when carrying out logistics services. Bredström and Rönnqvist (2008) made the earliest attempt to investigate the vehicle routing and scheduling problem with time windows and synchronized visits. Bredström and Rönnqvist (2008) presented a mathematical programming model and produced the first classical benchmark instances. After that, synchronized visits were extensively considered in VRP problems. Drexl (2012) conducted a survey, summarizing the classification of the VRP with synchronized visits. Quttineh et al. (2013) considered a model with the application to military aircraft mission planning, which is a further extension of the VRP with synchronized visits.

Haddadene et al. (2016) developed a A GRASP× ILS (iterated local search) algorithm to solve the benchmark instances given by Bredström and Rönnqvist (2008). Inspired from a practical application, En-nahli et al. (2016) studied the home health care problem by considering the synchronized visits. Decerle et al. (2018) designed a memetic algorithm to deal with the home health care problem considering synchronized visits. Hojabri et al. (2018) designed a large neighborhood search to solve the VRP with synchronized visits. Xu et al. (2018) applied the VRP with synchronized visits into the application of city logistics. Hu and Wei (2018) extended the VRP with synchronized visits by considering multi-vehicle and one-cargo instead of only vehicles.

Decerle et al. (2019) extended the study of Decerle et al. (2018) and optimized three different objective functions simultaneously. Haddadene et al. (2019) proposed a bi-objective mathematical model to minimize the workers' travel costs and maximize the customers' preferences for home health care considering the synchronized visits. Liu et al. (2019) investigated a vehicle routing problem with time windows and synchronized visits and proposed an adaptive large neighborhood search, which can obtain efficient solutions. Shao et al. (2019) investigated the logistics planning problem in e-commercial, considering synchronization and sliding time-window. Chu et al. (2019) considered the logistics synchronization in a regional scale. Anderluh et al. (2019a) addressed a new variant named two-echelon VRP with considering the impact of uncertainties and synchronization. Furthermore, Anderluh et al. (2019b) studied the multi-objective optimization of two-echelon VRP, considering synchronization.

On the basis of VRP with synchronization constraints, Li et al. (2020b) proposed a model with taking account of the split demand, multiple time window, as well as proportional service time. As an important contribution, a three-index based vehicle flow model and a set-covering model are formulated. Li et al. (2020a) considered a two-echelon VRP with synchronized visits, and CPLEX solver and an adaptive large neighborhood search algorithm were proposed to solve the model. Li et al. (2020c) investigated the VRP with synchronized visits in the applications of the prefabricated system, and an improved artificial bee colony is designed to solve the studied issue. The intensive comparison performed among the different meta-heuristic algorithms highlight the high effectiveness and efficiency of the proposed IABC. As an extension of the basic VRP with synchronization constraints, Frifita and Masmoudi (2020) studied a new model, abbreviated as VRPTW-TD-2MS, with taking into account temporal dependencies, multi-specialties, as well as multi-structures. The model was formulated as the mixed-integer programming, and three variable neighborhood search algorithms with different strategies are designed to solve the model.

2.3. VRP with uncertainty

In traditional logistics planning, decision-makers in the majority studies assume that the data is deterministic, but in real life, logistics practitioners always face a variety of uncertain data. Therefore, in order to obtain a more realistic model, more and more researchers have begun to consider the uncertain data in the model. RO is a powerful tool that deals with optimization problems with uncertainty factors. Agra et al. (2013) studied the VRP with time windows, which was the earliest work from the viewpoint of RO. Hu et al. (2018) studied the uncertainty of demand and travel times of VRP. Rodriguez et al. (2015) investigated the staff dimensioning in home health care with uncertain demands. Shi et al. (2017) studied the home health care routing problem in which they considered the time window and fuzzy demand. Naji et al. (2017) proposed a synchronized multiple traveling salesmen problem with time windows, then applied it to the home health care domain with considering the uncertain processing of caregivers and setup times. However, in their work, they dealt with the

Table 3
Previous studies of VRPs related to uncertain, greenhouse gas emissions and robust optimization.

Papers	Constraints					Modeling approach	
	uncertain demand	uncertain service time	uncertain travel time	synchronized visits	fuel consumption	stochastic programming	robust
Trautsamwieser et al. (2011)			✓				
Rodriguez et al. (2015)						✓	
En-nahli et al. (2016)				✓			
Shi et al. (2017)	✓	✓	✓				
Naji et al. (2017)		✓	✓	✓			
Shi et al. (2018b)	✓	✓			✓		
Decerle et al. (2018)			✓	✓			
Fathollahi-Fard et al. (2018)					✓		
Lin et al. (2018)							
Cappanera et al. (2018)	✓						✓
Shi et al. (2019)	✓	✓			✓	✓	✓
Peker et al. (2019)	✓	✓	✓				
Liu et al. (2019)				✓			
Haddadene et al. (2019)				✓			
Decerle et al. (2019)			✓	✓			
Fathollahi-Fard et al. (2019)					✓		
Grenouilleau et al. (2019)							
Bahadori-Chinibelagh et al. (2019)							
This study		✓	✓	✓	✓	✓	✓

✓denotes the context is covered.

uncertainty by proposing a MILP model. Although this article also claims that its model produces a robust solution, this article does not establish a model that strictly uses robust uncertain optimization. Shi et al. (2018b) modeled and solved simultaneous delivery and pick-up problem with stochastic travel and service times in home health care. Shi et al. (2019) proposed a robust model for a home health care routing and scheduling problem considering the uncertain travel and service times simultaneously. It is worth mentioning that, the study of Shi et al. (2019) has adopted two modeling approaches: RO and stochastic programming with recourse (SPR), and the comparison of their solutions empirically show that the solutions obtained by RO have stronger robustness than the solutions obtained by SPR. Recently, Hossein et al. (2019) investigated an operating room scheduling problem (ORSP) by taking into account stochastic duration, which can be viewed as a novel application of VRPS. Giallanza and Puma (2020) investigated a fuzzy green VRP in the domain of the agriculture food supply chain. In their model, the demand of the customers is assumed to be a fuzzy variable. Then the theory of fuzzy credibility is employed to build the formulations. Additionally, Ganji et al. (2020) addressed the heterogeneous fleet GVRP with the integration of the supply chain scheduling problem. A multi-objective optimization model is built, and three different types of heuristic: NSGA II, particle swarm optimization abbreviated as PSO, and artificial ant colony optimization are proposed to solve the model. Poonthalir et al. (2020) studied the mobile advertisement vehicle problem with considering the greenhouse emission, and a hierarchical optimization approach formulates the model. Finally, the optimal solution is obtained by a hybrid PSO with different stages. Fathollahi-Fard et al. (2020) investigated a bi-objective optimization framework for the variant of the home health care routing problem with considering the fuzzy environment. Finally, the proposed model is solved by a novel heuristic named social engineering optimizer.

The recent research involved in our research is summarized in Table 3.

After analyzing the aforementioned abundant literature, to the best of our knowledge, the main findings and literature gaps can be summarized as follows.

- Despite the great significance, the mathematical model for considering green VRP with uncertainties has not attracted enough attention. Furthermore, the green VRP with synchronized visits and uncertainties is rarely discussed and studied.
- Even though several heuristics have been designed to solve the VRP with synchronized visits, hybrid SA and TS algorithm has not been tried to solve the benchmark instances of Bredström and Rönnqvist (2008) and its variant model.
- The RO framework, which can enhance the robustness of the solutions, has not been employed as a modeling tool for developing a green VRP with synchronized visits.

To fill the aforementioned gaps and make this problem more practical, a robust optimization model for the green VRP with time window and synchronized visits considering GHG emission is proposed. Due to the feature of the model, different scenarios of robust optimization models are developed. Since the proposed model is NP-hard, a hybrid SA and TS algorithm is designed. Several series of experiments are conducted to analyze the efficiency of the proposed hybrid algorithm and the performance of the models.

3. Problem description and deterministic model

In this section, the assumptions of the RO-GVRPTWSyn are briefly introduced in subsection 3.1. Next, the basic notations used throughout this study are given in subsection 3.2. Then subsection 3.3 presents the fuel consumption model. Finally, a deterministic mathematical programming model is given in subsection 3.4.

3.1. Assumptions

In this study, it is assumed that there is a logistics company that has a depot. Each worker starts from the depot and returns to the depot after the journey. For the robust optimization model, it is assumed that the travel time between every two customers is uncertain, and the service time for each customer provided by the workers is also uncertain. Additionally, it is assumed that a certain number of customers require a service that needs two workers and qualifications to cooperate together simultaneously to finish the service. Each customer has a given time window.

3.2. Basic notations

The basic notations including input parameters and decision variables used through this study are listed as follows.

Input parameters:
Decision variables:

3.3. Computation of fuel consumption

Fuel consumption of vehicles is affected by various factors (Bektaş and Laporte, 2011), including travel distances, the weight of the vehicle, speed of the vehicle, engine type, road grade, inertia gravity, etc. Elhedhli and Merrick (2012) pointed out three main factors, which are travel distances, the weight of the vehicle, and the speed of the vehicle. For a specific vehicle, its parameters,

V:	Set of all vehicles.
K:	the number of available vehicles in set V.
C:	Set of all customers.
$\|C\|$:	the cardinality of set C.
N:	Set of all customers with two dummy customers (depots), namely $N = C \cup \{0\} \cup \{\|C\| + 1\}$.
i,j:	the index of the set N.
K:	the index of the set K.
Ω:	vehicle type.
$[a_i, b_i]$:	the time window for customer i. a_0 is the opening time of the depot.
FC_k:	the fixed cost for kth worker.
Q:	the maximum number of customers could be visited by each worker.
d_{ij}:	the distance between customer i and customer j.
c_{ij}:	the transportation cost between customer i and customer j.
t_{ij}:	the traveling time between customers i and j for a single trip.
s_i:	the service time for customer i.
P^{sync}:	the pairwise synchronized visits, where $P^{sync} \subset C \times C$.
λ:	denotes the factor converting the fuel rate (grams per second to liters per second).
f_c:	the fuel and CO_2 emissions cost per liter ($).
E	heating value of typical bio-diesel fuel (kilo-joules per gram).
ξ:	fuel-to-air mass ratio.
ϱ:	drive train efficiency.
τ:	acceleration (m/second^2).
μ:	Air density (kilogram/meter 3).
∂:	efficiency parameter for bio-diesel engines.
θ_{ij}:	road angle between i and j.
C_c:	coefficient of rolling resistance.
C_d^t:	coefficient of rolling drag.
R^t:	frontal surface area of the vehicle ($meter^2$).
M^t:	vehicle mass (kilogram).
H^t:	engine friction factor (kilo-joules per revolution per liter).
F^t:	engine speed (revolution per second).
D^t:	engine displacement (liters).
B:	a large number, which is used to construct the objective function.
Λ_k:	speed of vehicle k.

x_{ijk} :	if vehicle k travels from node i to node j, in which $i \neq j$, $x_{ijk} = 1$. Otherwise, $x_{ijk} = 0$.
u_{ik} :	the beginning service time of customer i for vehicle k.

Table 4
Specific parameters of vehicles (Masmoudi et al., 2018).

Parameters	Type 1 (ω = 1)	Type 2 (ω = 2)	Type 3 (ω = 3)
M^{ω}	1592	1845	2095
R^{ω}	2.12	2.51	2.35
C_d^{ω}	0.28	0.25	0.34
F^{ω}	66.66	63.33	65.50
H^{ω}	0.38	0.50	0.85
D^{ω}	2.0	2.1	3.0

including frontal surface area, vehicle mass, engine friction factor, engine speed, engine displacement, etc. are constant values. Table 4 shows the specific parameters of three different types of vehicles (Masmoudi et al., 2018).

Inspired from the idea proposed by Bektaş and Laporte (2011), the fuel consumption is computed by equation (1), which shows as follows:

$$FuelCost_{ijk} = \frac{v_k \xi f_c H^{\omega} F^{\omega} D^{\omega} d_{ij}}{e\lambda} + \frac{\xi f_c d_{ij} v_k^2 (0.5\mu R^{\omega} C_d^{\omega})}{1000\varrho\partial e\lambda} + \frac{\xi f_c M^{\omega} (\tau sin(\theta_{ij}) g C_c cos(\theta_{ij}) g) d_{ij} x_{ijk}}{1000\varrho\partial e\lambda} \quad (1)$$

in which, g is the gravitational constant (9.81 m/s^2).

The fuel consumption equation (1) is a nonlinear function,

$$FuelCost_{ijk} = \frac{\Lambda_k(\xi=1)(f_c=1.616)H^{\omega}F^{\omega}D^{\omega}d_{ij}}{(e=41.5)(\lambda=737)} + \frac{(\xi=1)(f_c=1.616)d_{ij}\Lambda_k^2(0.5(\mu=1.2041)R^{\omega}C_d^{\omega})}{1000(\varrho=0.45)(\partial=0.9)(e=41.5)(\lambda=737)} + \frac{(\xi=1)(f_c=1.616)M^{\omega}((\tau=0)sin(0^o)(g=9.81)(C_c=0.01)cos(0^o)(g=9.81))d_{ij}x_{ijk}}{1000(\varrho=0.45)(\partial=0.9)(e=41.5)(\lambda=737)} \quad (2)$$

which has been widely used in pollution-routing problem (Bektaş and Laporte, 2011). In this study, the parameter setting of θ_{ij} is from the article of Masmoudi et al. (2018), who assumed that the θ_{ij} equals to zero. The petrol price ($f_c = 1.616$) is according to the data provided by https://www.globalpetrolprices.com/United-Kingdom/gasoline_prices/.

$$FuelCost_{ijk} = 0.00005283549\Lambda_k H^{\omega}F^{\omega}D^{\omega}d_{ij} + \frac{0.9729128 d_{ij}\Lambda_k^2(R^{\omega}C_d^{\omega})}{12387127.5} + \frac{15.85296 M^{\omega} d_{ij} x_{ijk}}{12387127.5} \quad (3)$$

After replacing the input constant parameters, then the above equation can be derived as follow:

As mentioned before, different types of vehicles have different specified parameters. In this study, three different types of vehicles are considered, and the specified parameters show in Table 4. Therefore, the formulation (3) is used to calculate the fuel cost after replacing the specified parameters of each type of vehicle, which is used to measure the GHG.

3.4. Deterministic model

Motivated by Bredström and Rönnqvist (2008), a simple idea of building the VRP with synchronization visit constraints model is to treat the customer who needs synchronization services as two customers with the same geographic and time windows, and one of these two customers is a dummy customer. Although the idea is simple, the complexity of the problem has greatly increased. Regarded as a further extension of Bredström and Rönnqvist (2008), the deterministic mathematical programming with constraints can be formulated as follows.

$$\min h = \underbrace{\sum_{k\in V}\sum_{j\in C} x_{0jk} FC_k}_{\text{fixed cost of vehicles}} + \underbrace{\sum_{k\in V}\sum_{i\in N}\sum_{j\in N} FuelCost_{ijk}}_{\text{fuel consumption cost}} + \underbrace{\sum_{k\in V}\sum_{i\in N}\sum_{j\in N} c_{ij} x_{ijk}}_{\text{travel cost of vehicle}} \quad (4)$$

The objective function (4) aims at minimizing total travel cost, fuel consumption cost, and the fixed cost of workers.

In this study, it is assumed that each customer requires service in a certain period. The constraint (5) ensures that each customer is visited only once by a worker.

$$\sum_{k\in V}\sum_{j\in N} x_{ijk} = 1, \forall i \in C, \quad (5)$$

After visiting a customer, the worker will visit the next customer or return to the depot. Hence, there is a flow conversion constraint that shows in constraint (6) to guarantee that a worker leaves the customer after visiting customer i.

$$\sum_{j\in N} x_{ijk} - \sum_{j\in N} x_{jik} = 0, \forall i \in C; k \in V, \quad (6)$$

Each worker starts from the depot. After finishing all the customers, the worker must return to the depot. Constraints (7)–(8) represent that each worker starts from the depot, and return to the depot after visiting several customers.

$$\sum_{j\in C} x_{0jk} \le 1, \forall k \in V, \tag{7}$$

$$\sum_{j\in C} x_{j(n+1)k} \le 1, \forall k \in V, \tag{8}$$

Constraint (9) ensures that synchronized visits start simultaneously.

$$\sum_{k\in K} u_{ik} = \sum_{k\in K} u_{jk}, \forall (i,j) \in P^{sync} \tag{9}$$

Constraints (10)–(11) ensure that the service is done in the time windows $[a_i, b_i]$, which is the available for customer i. The explanation of constrains (10)–(11) can be referred to Kolen et al. (1987).

$$u_{ik} + s_i + d_{ij} \Big/ \Lambda_k - B\left(1 - x_{ijk}\right) \le u_{jk}, i,j \in N; k \in V, \tag{10}$$

$$a_i \le u_{ik} \le b_i, i \in N; k \in V, \tag{11}$$

Finally, the constraints (12) represent that these decision variables are continuous real numbers and binary.

$$x_{ijk} \in \{0,1\}, u_{ik} \ge 0, i,j \in N, k \in V, \tag{12}$$

4. Robust optimization model

4.1. The sets of uncertainties

Before presenting the RO-GVRPTWSyn model, the uncertainty sets of travel and service times are introduced. The detailed definition of the uncertainty set is introduced by Ben-Tal and Nemirovski (1999). For a given worker k, two uncertainties sets are defined. The first one is the uncertain service time (UST) $\mathbb{U}_s^k$, and another one is the uncertain travel time (UTT) set $\mathbb{U}_t^k$ (Hu et al., 2018; Wu et al., 2017). In our study, $\check{t}_{ij}$ illustrates that the travel time between each paired nodes (i,j), is with respect to UTT set $\mathbb{U}_t^k$. Additionally, $\check{t}_i$ are defined that the service time for customer i is belonged to UST set $\mathbb{U}_s^k$. The detailed UST and UTT sets are presented in formulation (13) and (15).

$$U_s^k = \left\{ \check{t}_i \in R^{|N^k|} \middle| \check{t}_i = \overline{t_i} + \alpha_i \widehat{t}_i, \sum_{i\in N^k} \left|\alpha_i\right| \le \Gamma_s^k, \left|\alpha_i\right| \le 1, \Gamma_s^k = \left[\theta_s \middle| N^k \right| \times \right], \forall i \in N^k \right\} \tag{13}$$

$$\mathbb{U}_s = \times_{k\in K} U_s^k \tag{14}$$

As shown in formulation in (14), $\mathbb{U}_s$ is a set for describing all the USTs of customers. In the formulation in (13), N^k represents a set that is composed of whole the customers serviced by work k. The UST for customer i is represented by $\check{t}_i$, while its average value equals to $\overline{t_i}$. α_i is regarded as an auxiliary variable for help describing the set. Γ_s^k is a variable for controlling the level of the UST, and it is defined on the basis of the budget uncertainty (Hu et al., 2018). $\theta_s \in [0,1]$ is a coefficient in the UST budget. $[\theta_s \left| N^k \right|]$ is the Gauss function of $\theta_s \left| N^k \right|$.

$$U_t^k = \left\{ \check{t}_{ij} \in R^{|A^k|} \middle| \check{t}_{ij} = \overline{t_{ij}} + \beta_{ij} \widehat{t}_{ij}, \sum_{(i,j)\in A^k} \left|\beta_{ij}\right| \le \Gamma_t^k, \left|\beta_{ij}\right| \le 1, \Gamma_t^k = \left[\theta_t \middle| A^k \right| \times \right], \forall (i,j) \in A^k \right\} \tag{15}$$

$$\mathbb{U}_t = \times_{k\in K} U_t^k \tag{16}$$

Similar to equation (14), in formulation (16), $\mathbb{U}_s$ is a set for describing all the UTTs on the road. In the formulation in (15), A^k represents a set which is composed by whole the arcs/roads serviced by worker k. The UTT between a paired customers i and j is represented by $\check{t}_{ij}$, while its average value equals to $\overline{t_{ij}}$. β_{ij} is regarded as an auxiliary variable for constructing the set. Γ_s^k is a variable for controlling the level of the UTT, and it is defined on the basis of the budget uncertainty (Hu et al., 2018). $\theta_t \in [0,1]$ is a coefficient in the UTT budget. $[\theta_t \left| A^k \right|]$ is the Gauss function of $\theta_t \left| A^k \right|$.

4.2. RO-GVRPTWSyn model

In the deterministic VRP models, the constraints of time-windows greatly impact the feasibility of the solutions (Solomon, 1987). While, in the RO-GVRPTWSyn model, the constraints of UST and UTT make this issue more complicated, since that our RO-GVRPTWSyn attempts to find the optimal (or near-optimal) solutions which are feasible for any scenarios. However, it should also be noticed that if all the cases of possible uncertainties are considered, there will be a big expense in computing and exploring space. According to the latest research (Hu et al., 2018), a trade-off between the exploring uncertainties and computation performance is considered. In section 4.1, the sets of UST and UTT, which are independent with routes, are defined. In the RO-GVRPTWSyn model, UST and UTT constraints will replace the corresponding constraints in the deterministic model. The RO-GVRPTWSyn is defined in the formulations (17)–(19).

$$\min \sup_{s\in ext(\mathbb{U}_s), t\in ext(\mathbb{U}_t)} \underbrace{\sum_{k\in V}\sum_{j\in C} x_{0jk} FC_k(s,t)}_{\text{fixedcostofvehicles}} + \underbrace{\sum_{k\in V}\sum_{j\in N}\sum_{i\in N} FuelCost_{ijk}(s,t)}_{\text{fuelconsumptioncost}} + \underbrace{\sum_{k\in V}\sum_{j\in N}\sum_{i\in N} c_{ij} x_{ijk}(s,t)}_{\text{travelcostofvehicle}} \tag{17}$$

subject to:
Constraints (5)–(9),

$$\check{s}_{ik}(s,t) + t_i + t_{ij} - M\left(1 - x_{ijk}\right) \le \check{s}_{jk}(s,t), \forall k \in V; i,j \in N, s \in ext(\mathbb{U}_s), t \in ext(\mathbb{U}_t), \tag{18}$$

$$a_i \le \check{s}_{ik}(s,t) \le b_i,\ \forall k \in V; i \in N; s \in ext(\mathbb{U}_s), t \in ext(\mathbb{U}_t), \tag{19}$$

In the objective function (17), $ext(\mathbb{U}_s)$ and $ext(\mathbb{U}_t)$ include all the extreme points of UST and UTT sets $\mathbb{U}_s$ and $\mathbb{U}_t$, respectively. Formulation (17) minimizes the total cost, including the travel cost and fuel cost, among the worst cases. Constraints (18)–(19) are the time-window constraints that involved UST and UTT. The rest constraints are from the deterministic model.

In the proposed heuristic algorithm, infeasible solutions for time windows are allowed, since it is helpful to overcome the shortcomings of local optimum. In the traditional deterministic VRPTW model Solomon (1987), one can directly utilize the delay time as a penalty value to add to the objective function as the revised objective function. But in robust models, this problem becomes much more complicated, since minimizing the objective function in the worst cases should be considered. Here a concept of the Largest Possible Arrival Time (LPAT), which has also been adopted by Hu et al. (2018); Shi et al. (2019), is introduced to get the penalty value. In case that the LPAT is higher than the due time for a specific customer, then a penalty will be added to the objective function; otherwise, there is no penalty generated.

Let r_k be the set of all the vertices (including customers and the depot) in route k, and $n_k = |r_k|$ represent the cardinality of r_k. Additionally, the route could be described as: $r_k = \{v_0 = \text{depot}, v_1, \ldots, v_j, \ldots v_{n_k}, v_{n_k+1} = \text{lab}\}$, and v_j is the jth vertex in r_k. In case that the solutions must follow constraints (18), which can be written detailed as equation (20).

$$\check{S}_{v_{j+1}} = \max\left(\check{S}_{v_j} + \check{t}_{v_j v_{j+1}} + \check{t}_{v_j}, a_{v_{j+1}}\right). \tag{20}$$

Let $\mathscr{T}^k(v_i, \Gamma_s^k, \Gamma_t^k)$ be the LPAT for v_i with the parameters Γ_s^k and Γ_t^k. Now, the LPAT can be written as a recursive function (23). Three robust optimization scenarios are taking into account. In the first one, $\Gamma_t^k = 0$, which means that LPAT is only for UST (LPAT-OUST), without considering UTT. This can be expressed as formulation (21). The LAPT only for UTT (LPAT-OUTT) is formulated as equation (22). Additionally, The LPAT for considering both UTT and UST (LPAT-UTTAST) is derived as formulation (23).

Let R represent the schedule of routes, which can be viewed as a solution of the problem. $obj(R)$ in (24) is a objective function for evaluating the schedule R. In the objective function (24), $h(R)$ is obtained by the formulation (4), and $\mathfrak{M}$ is a coefficient for the penalty where the constraints of time window is violated.

$$obj(R) = h(R) + \mathfrak{M} \sum_{k \in K} \sum_{i=1}^{|r_k|} \max\left(0, \mathscr{T}^k\left(v_i, \Gamma_s^k, \Gamma_t^k\right) - b_{v_i}\right) \tag{24}$$

$$\mathscr{T}^k\left(v_i, \Gamma_s^k, \Gamma_t^k\right)|_{\Gamma_t^k=0} = \begin{cases} 0 & i = 0, \\ \max(a_{v_i}, \mathscr{T}_{v_{i-1}} + \bar{t}_{v_{i-1}v_i} + \overline{t_{v_{i-1}}}) & 1 \le i \le n, \Gamma_s^k = 0; \\ \max\left(a_{v_i}, \mathscr{T}^k\left(v_{i-1}, \Gamma_s^k - 1, 0\right) + \bar{t}_{v_{i-1}v_i} + \hat{t}_{v_{i-1}} + \overline{t_{v_{i-1}}}, \mathscr{T}^k\left(v_{i-1}, \Gamma_s^k, 0\right) + \bar{t}_{v_{i-1}v_i} + \overline{t_{v_{i-1}}}\right) & 1 \le i \le n, \Gamma_s^k > 0; \\ \mathscr{T}^k\left(v_i, \Gamma_s^k - 1, \Gamma_t^k\right)\Gamma_s^k > i, -\infty & otherwise \end{cases} \tag{21}$$

$$\mathscr{T}^k\left(v_i, \Gamma_s^k, \Gamma_t^k\right)|_{\Gamma_s^k=0} = \begin{cases} 0 & i = 0, \\ \max(a_{v_i}, \mathscr{T}_{v_{i-1}} + \bar{t}_{v_{i-1}v_i} + \overline{t_{v_{i-1}}}) & 1 \le i \le n, \Gamma_t^k = 0; \\ \max\left(a_{v_i}, \mathscr{T}^k\left(v_{i-1}, 0, \Gamma_t^k - 1\right) + \bar{t}_{v_{i-1}v_i} + \hat{t}_{v_{i-1}v_i} + \overline{t_{v_{i-1}}}, \mathscr{T}^k\left(v_{i-1}, 0, \Gamma_t^k\right) + \bar{t}_{v_{i-1}v_i} + \overline{t_{v_{i-1}}}\right) & 1 \le i \le n, \Gamma_t^k > 0; \\ \mathscr{T}^k\left(v_i, \Gamma_s^k, \Gamma_t^k - 1\right)\Gamma_t^k > i, -\infty & otherwise \end{cases} \tag{22}$$

$$\mathscr{T}^k\left(v_i,\Gamma_s^k,\Gamma_t^k\right)=\begin{cases}0 & i=0,\\ \max(a_{v_i},\mathscr{T}_{v_{i-1}}+\bar{t}_{v_{i-1}v_i}+\overline{t_{v_{i-1}}}) & 1\le i\le n,\Gamma_t^k=\Gamma_s^k=0;\\ \max\left(a_{v_i},\mathscr{T}^k\left(v_{i-1},0,\Gamma_t^k-1\right)+\bar{t}_{v_{i-1}v_i}+\hat{t}_{v_{i-1}v_i}+\overline{t_{v_{i-1}}},\mathscr{T}^k\left(v_{i-1},0,\Gamma_t^k\right)+\bar{t}_{v_{i-1}v_i}+\overline{t_{v_{i-1}}}\right) & 1\le i\le n,\Gamma_s^k=0,\Gamma_t^k>0;\\ \max\left(a_{v_i},\mathscr{T}^k\left(v_{i-1},\Gamma_s^k-1,0\right)+\bar{t}_{v_{i-1}v_i}+\hat{t}_{v_{i-1}}+\overline{t_{v_{i-1}}},\mathscr{T}^k\left(v_{i-1},\Gamma_s^k,0\right)+\bar{t}_{v_{i-1}v_i}+\overline{t_{v_{i-1}}}\right) & 1\le i\le n,\Gamma_t^k=0,\Gamma_s^k>0;\\ \max\left(a_{v_i},\mathscr{T}^k\left(v_{i-1},\Gamma_s^k-1,\Gamma_t^k-1\right)+\bar{t}_{v_{i-1}v_i}+\hat{t}_{v_{i-1}v_i}+\overline{t_{v_{i-1}}}+\hat{t}_{v_{i-1}},S^k\left(v_{i-1},\Gamma_s^k,\Gamma_t^k\right)+\bar{t}_{v_{i-1}v_i}+\overline{t_{v_{i-1}}},\mathscr{T}^k\left(v_{i-1},\right.\right. & \\ \left.\left.\Gamma_s^k-1,\Gamma_t^k\right)\right. & 1\le i\le n,\Gamma_s^k>0,\Gamma_t^k>0;\\ \mathscr{T}^k\left(v_{i-1},\Gamma_s^k,\Gamma_t^k-1\right)+\bar{t}_{v_{i-1}v_i}+\hat{t}_{v_{i-1}v_i}+\overline{t_{v_{i-1}}}\right) & \\ \mathscr{T}^k\left(v_i,\Gamma_s^k-1,\Gamma_t^k\right) & \Gamma_s^k>i,\\ \mathscr{T}^k\left(v_i,\Gamma_s^k,\Gamma_t^k-1\right)\Gamma_t^k>i,-\infty & \\ & otherwise\end{cases} \tag{23}$$

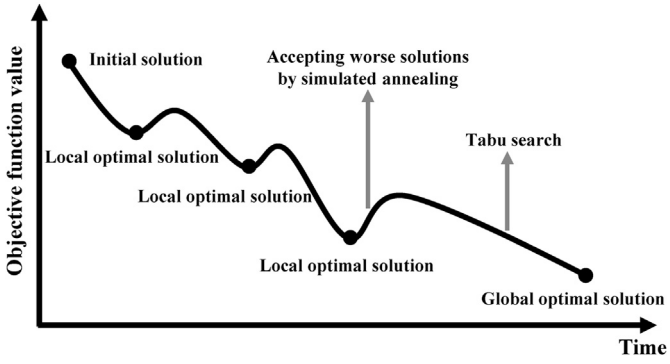

Fig. 2. A graphical interpretation of perturb operation and candidate acceptance.

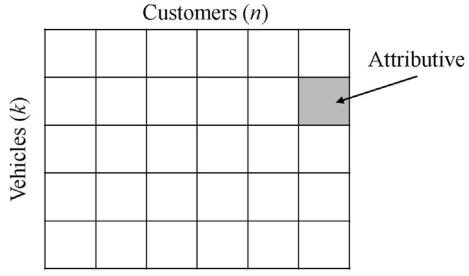

Fig. 3. The structure of *TL*(Shi et al., 2020).

5. Proposed approaches

The RO-GVRPTWSyn model itself is an NP-hard problem, which is a challenge for obtaining optimal solutions. Considering the synchronized visits of workers in this study will lead the problem more intractable. Therefore, a heuristic algorithm is considered in our research for solving the proposed models. Simulated annealing (SA) is an efficient approach for dealing with combinatorial optimization problems (Kirkpatrick et al., 1983). One of the critical features of the SA algorithm is that it can guide the exploring process to get rid of local optimum by utilizing the strategy of allowing in accepting bad solutions in the traditional hill-climbing moves. Tabu search, initially proposed by Glover (1989, 1990), is also a widely used meta-heuristic algorithm with taking into account the taboo rules into local search.

According to our trials, SA usually has strong global search ability while shows less local search ability. Meanwhile, TS has an excellent performance in local search ability. Therefore, the hybrid SA and TS can boost the performance of the searching ability both globally and locally. This study makes the first attempt to design a hybrid SA and TS for solving VRP with synchronization. Fig. 2 shows a graphical interpretation of the process of the hybrid SA with tabu search. Our heuristic starts from an initial solution s_0, then hybrid SA and TS are adopted to improve the solution. The algorithm stops until the terminal conditions are reached. This section mainly presents the detailed procedures of the proposed algorithm.

5.1. Greedy algorithm for generating an initial solution

The initial solution is critical to the convergence time of the meta-heuristics. A better initial solution can significantly speed up the convergence of the meta-heuristics. A completely randomly generated initial solution often has the characteristics that the objective function is large and not feasible. A simple and effective greedy algorithm for generating the initial solution is newly designed in this section. The proposed greedy algorithm can be decomposed into two phases.

The first phase is described in Algorithm 1. In this step, the synchronization constraint is ignored, and the routes s_0 are generated according to the classical Push Forward Insertion Heuristic (PFIH) method, which is initially proposed by Solomon (1987) for solving the classical VRPTW. After that, in the second step, as shown in Algorithm 2, the s_0 is repaired by taking full consideration of the synchronization constraints.

Algorithm 1. First phase: generate a basic solution.

```
Input: V
pool ← V ;                                   // the pool denotes the whole customers.
tour ← null ;                                // tour represents a route.
routes ← null ;                              // routes illustrates a solution.
S ← Initialization() ;                       // S denotes the incumbent solution.
S* ← S ;                                     // S* indicates the best solution found so far.
k=0;
while (|pool| > 0) do
    A node v of customer is selected according to Solomon's criteria.
    if pair(v) is not in the current tour then
        if v can be inserted to the current tour then
            Insert v to the tour to the right position i according to Solomon's criteria.
            update the time window tour(j), where j > i;
            update tour; update the pool ← pool \ v.
        end
        else
            routes(k) ← tour
            tour ← null
            k ← k + 1
        end
    end
end
if |tour| > 0 then
    routes(k) ← tour
end
Return routes;
```

Algorithm 2. Second phase: repair the time window.

```
input: routes, pairs.
pairs_pool ← paris
while |pairs_pool| > 0 do
    v1 ← pairs(1); // pairs is a set for storing the information of the customers who demand
       synchronized services
    v2 ← pair(v1);// pair is a function for finding the corresponding synchronized services
    (k1, i) ← finding the index of the tour where v1 located in.
    (k2, j) ← finding the index of the tour where v2 located in.
    t_{k1,i} ← max(t_{k1,i}, t_{k2,j})
    t_{k2,j} ← max(t_{k1,i}, t_{k2,j})
    update t_{k1,h}, where h > i;
    update t_{k2,l}, where l > j;
    remove v1 and v2 from pairs_pool;
    update pairs_pool.
end
s_0 ← routes
Return s_0 ;
```

5.2. Hybrid simulated annealing and tabu search

5.2.1. Neighborhood search operators

Neighborhood structure plays an essential role in meta-heuristics, especially for complex combinatorial optimization problems. In this study, different types of neighborhood search operators, including the relocate, insert, swap, 2-opt operators, and $\lambda-$ interchange ($\lambda = 2$) are adopted.

5.2.2. Tabu list

Tabu list, abbreviated as TL, records the moves of customers in the neighborhood search process. A good tabu list and tabu rule can avoid appearing cycled solutions in a short memory of the searching process. In this study, the move operations are summarized as two different categories: the moved customers are located in different routes; the moved customers are located in the same route.

Let us assume that an instance with the number of clients is n, and the number of vehicles (or workers) is k. Then the TL is represented by a $n \times k$ matrix. The value showed in the element $TL(i,j)$ denotes the forbidden times of movement for inserting customer i to vehicle j. Fig. 3 gives an example of the structure of TL.

5.2.3. Diversification

Diversification is another essential operator for guiding the searching process to a new exploring region, and this benefit the TS git rid of the local optimum. The strategy of diversification is also successfully applied in the literature (Shi et al., 2019).

In this study, the diversification operator is implemented by giving a penalty to the moves which are frequently adopted. The frequency list (FL) is a table for storing the information involved the frequency of any moves, and FL is updated in each iteration. s represents a solution which is located in the neighborhood of $s^{current}$, and P is a set including all the possible moves that can be taken by $s^{current}$. $\mathscr{M}$ means the move from $s^{current}$ to s. $g(s^{current}, \mathscr{M})$ presents how many times the move have been executed previously. λ is a number of the current iterations. $\eta \in [0,1]$ is a real number that randomly generated. The current objective function $obj(s)$ is rewritten as $obj'(s)$ which is expressed in equation (25).

$$obj'(s) = obj(s)\left(1 + \eta \sum_{\mathscr{M} \in P} g(s^{current}, \mathscr{M}) \Big/ \lambda\right), \tag{25}$$

5.2.4. Route refinement

Route refinement operation is a widespread technique to improve the solutions VRP. In this study, the 2-opt, 3-opt, inverse operators are adopted as route refinement mechanism, that is implemented to each route every n_r iterations.

5.2.5. The main procedures of the hybrid SA and TS

After presenting the detailed operators in the aforementioned

Table 5
The feature of the different types of time windows (TW).

Type of TW	Feature of TW	Example [E,L]
F	The beginning service time is fixed, and the length of client's TW is 0.	E = 10; L = 10
S	The length of client's TW is small.	E = 10; L = 12
M	The length of client's TW is medium.	E = 10; L = 20
L	The length of this TW is large.	E = 10; L = 40
A	There is no TW restrictions for a and b.	E = 10; L = 80

Table 6
Main parameters utilized in our study.

Items	introduction of parameters	Values
Equation (24)	$\mathfrak{M}$: a coefficient of the penalty	100000
SA	T_0: the initial value of temperature.	100
	T_F: the threshold of temperature	0.1
	ζ: the Boltzmann's Constant value.	0.995
TS	η: the parameter in the diversification	0.2
	n_{TL} : the size of TL	round ((size of the instance)*0.4)

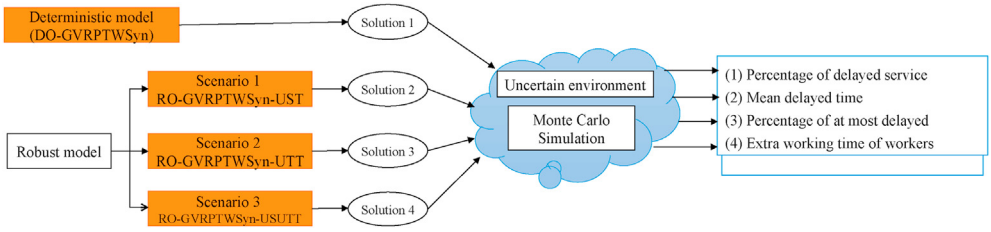

Fig. 4. The main procedures of the Monte Carlo Simulation for evaluating the solutions.

$V_i(i = 0,1,2,3)$:.	The percentage of at most i customers receive delayed service. Especially, v_0 indicates the scenario that non customer receives delayed service.
PDS:	The percentage of delayed services for customers.
MDT:	The mean delayed time for those clients who have received delayed services.
MET:	The mean extra working time for the delivery man.

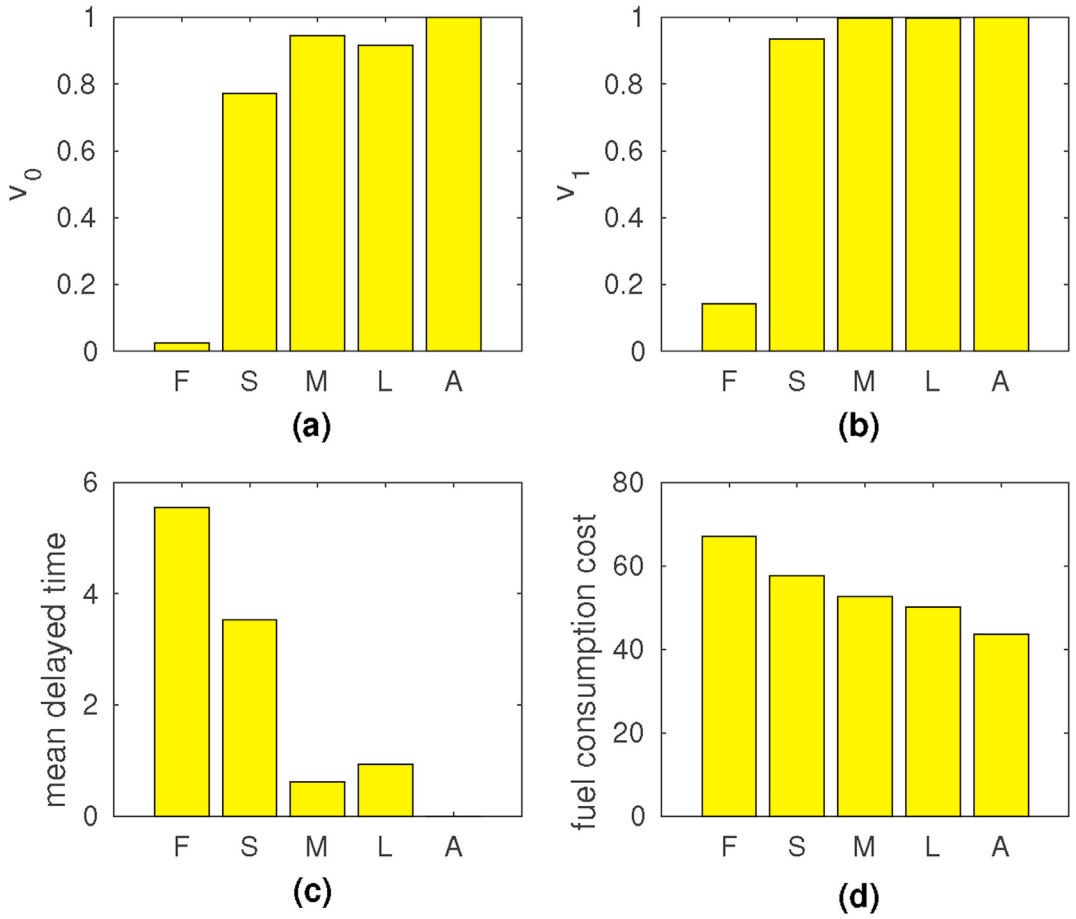

Fig. 5. The bar-plots for the average values of v_0, v_1, MDT, and the amount of fuel consumption cost.

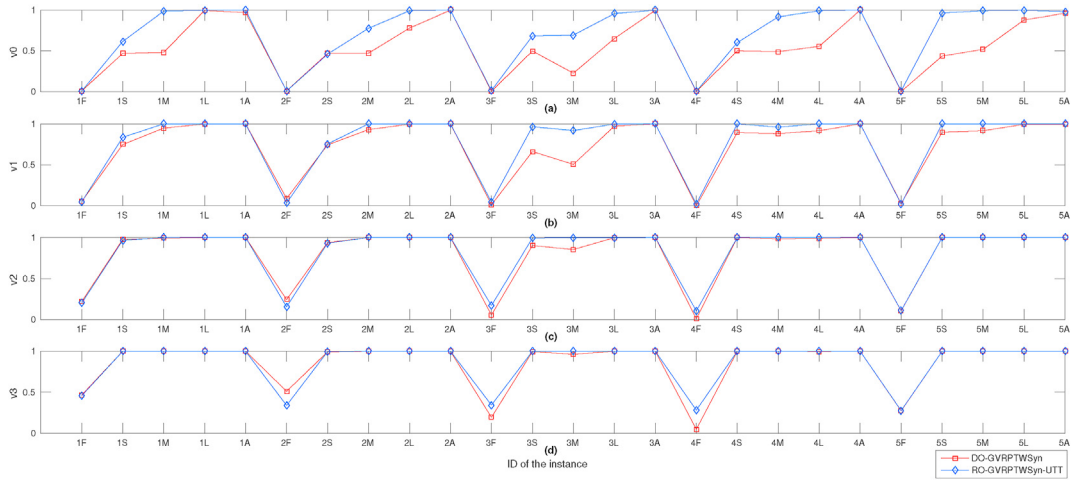

Fig. 6. The simulated v_i indicators for the solutions obtained by DO-GVRPTWSyn and RO-GVRPTWSyn-UTT.

sections, this section shows the pseudo of the hybrid SA and TS. T_0 represents the initial temperature. At the beginning of the algorithm, S, a feasible solution, is produced by adopting the procedures of 5.1. For each loop, a newly solution S' is generated from S by applying several neighborhood operators. This move from S to S' should follow the rules of TS. Let obj(s_1) represent the function for evaluating s_1. Δ represents the gap value between obj(s_1) and obj(s_2).

Algorithm 3. Framework of the proposed Hybrid SA with tabu

search.

different scenarios of robust models are addressed. To further analyze the feature of the solutions, the Monte Carlo simulation

Input all the initial parameters: T_0, T_F, ζ and $Iter_{MAX}$;
$T \leftarrow T_0$; // T denotes the current temperature;
$Iter \leftarrow 0$; // $Iter$ reprsents iteration;
$S \leftarrow$ Initialization() ; // S indicates the incumbent solution;
$S^* \leftarrow S$; // S^* illustrates the best solution;
Update tabu list (S);
while ($T \geq T_F$) **do**
  $Iter \leftarrow Iter + 1$;
  $S^{'} \leftarrow$ Neighborhood operation(S);
  $\Delta \leftarrow f(S^{'}) - f(S^{)}$;
  if $\Delta < 0$ **then**
    $S \leftarrow S^{'}$;
    Update tabu list (S);
  else
    r $\leftarrow$Random(0, 1) **if** $r < exp(-\Delta/T)$ **then**
      $S \leftarrow S^{'}$;
      Update tabu list (S);
    end
    if $f(S^*) > f(S)$ **then**
      $S^* \leftarrow S$; // update the current best solution
    end
    if $Iter >= Iter_{MAX}$ **then**
      $T \leftarrow \zeta * T$; // update the current temperature
      $Iter \leftarrow 0$;
    end
  end
end
Output the best solution S^*;

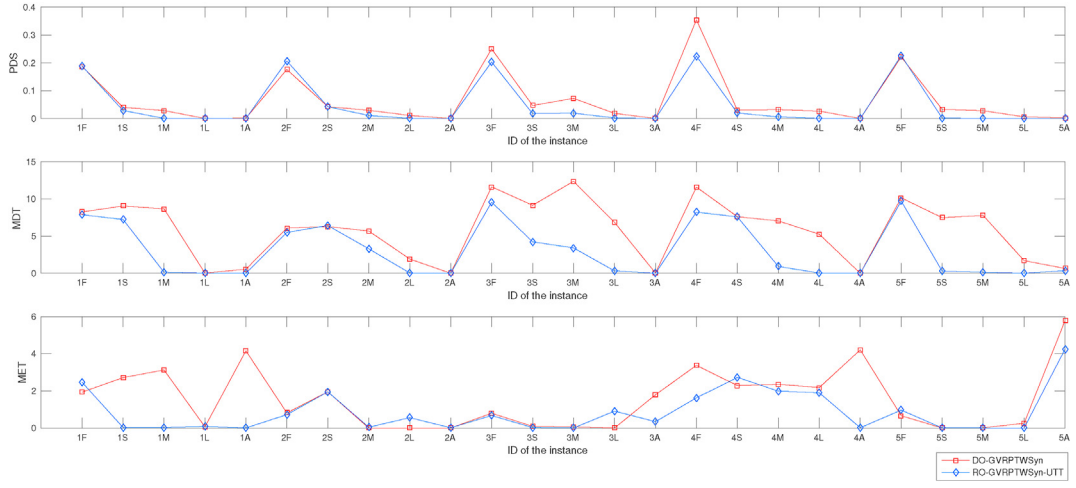

Fig. 7. MET, PDS, MDT for the solutions obtained by DO-GVRPTWSyn and RO-GVRPTWSyn-UTT.

6. Experiments

This section mainly presents comprehensive experiments performed to evaluate the models and solving approach proposed in this study. (1) The validity of the designed approach in Algorithm 3 is verified by solving the deterministic model with the broadly used benchmark instances of Bredström and Rönnqvist (2008). (2) The method is employed to obtain the robustness indicators. How the length of time windows affect the performance of robustness and greenhouse gas emissions are also discussed. (3) Intensively comparisons among the different solutions produced from the deterministic model and the different robust models are performed. (4) A sensitivity analysis with the different types of vehicles is carried out. (5) Statistical analysis is performed to validate the differences

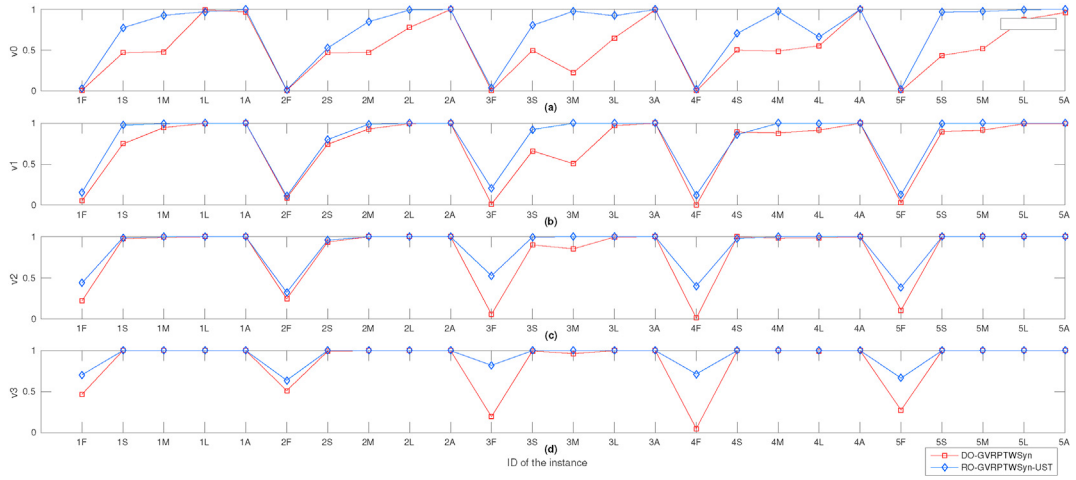

Fig. 8. The simulated v_i indicators for the solutions obtained by DO-GVRPTWSyn and RO-GVRPTWSyn-UST.

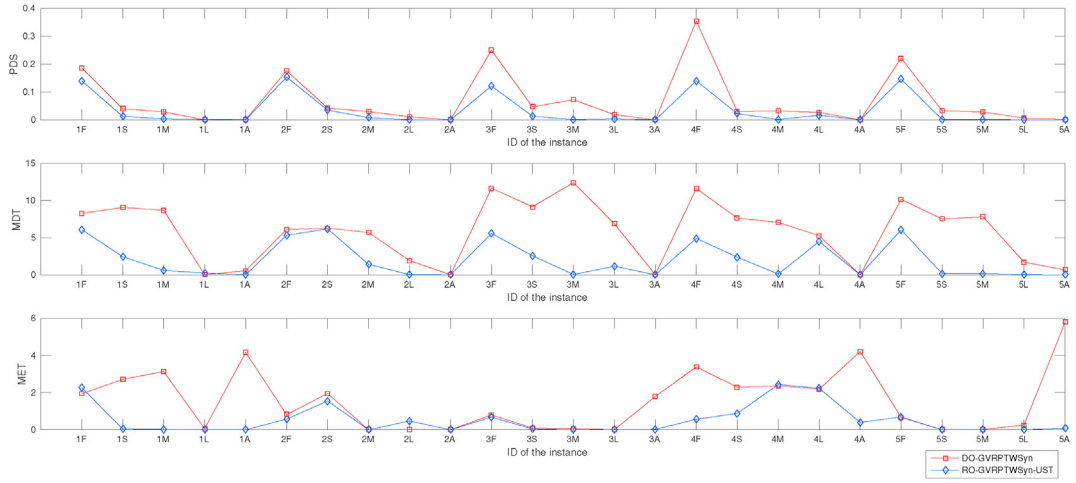

Fig. 9. MET, PDS, MDT for the solutions obtained by DO-GVRPTWSyn and RO-GVRPTWSyn-UST.

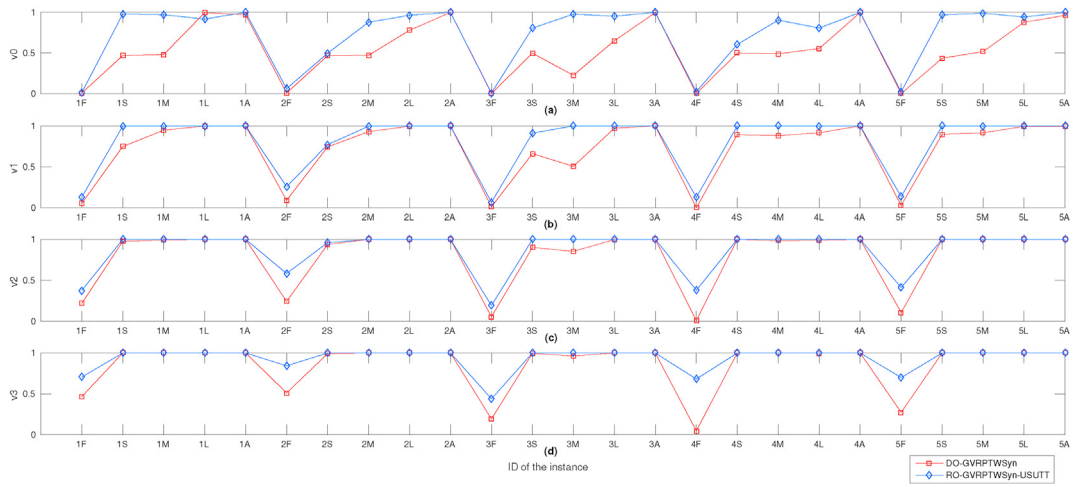

Fig. 10. The simulated v_i indicators for the solutions obtained by DO-GVRPTWSyn and RO-GVRPTWSyn-USUTT.

among the models. (6) The trade-off between the GHG emissions and robustness indicators is discussed via the Pareto-based bi-objective optimization models.

The algorithm used in this study is coded with JAVA programming language and executed on the Ubuntu 18.04 system.

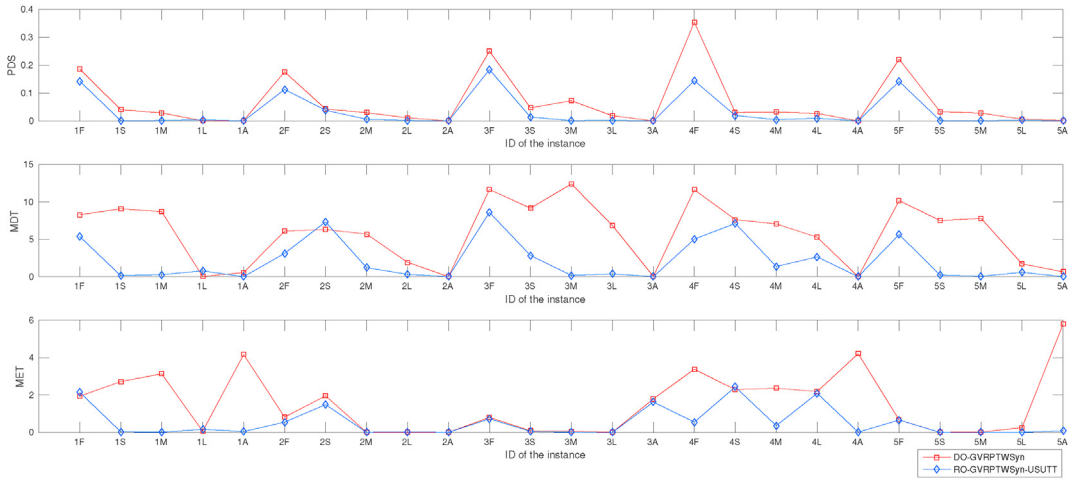

Fig. 11. MET, PDS, MDT for the solutions obtained by DO-GVRPTWSyn and RO-GVRPTWSyn-USUTT.

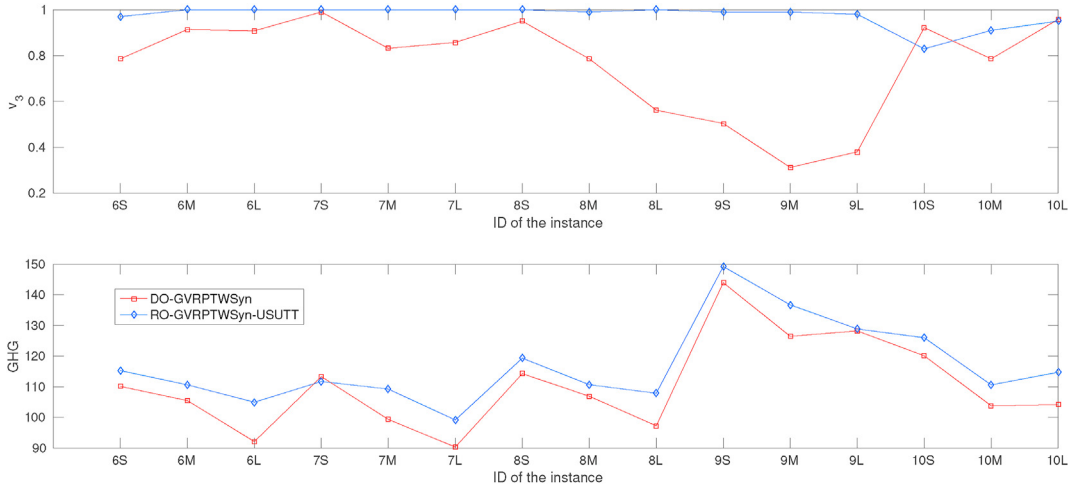

Fig. 12. v_3 and fuel consumption cost for the solutions obtained by DO-GVRPTWSyn and RO-GVRPTWSyn-USUTT in large size instances.

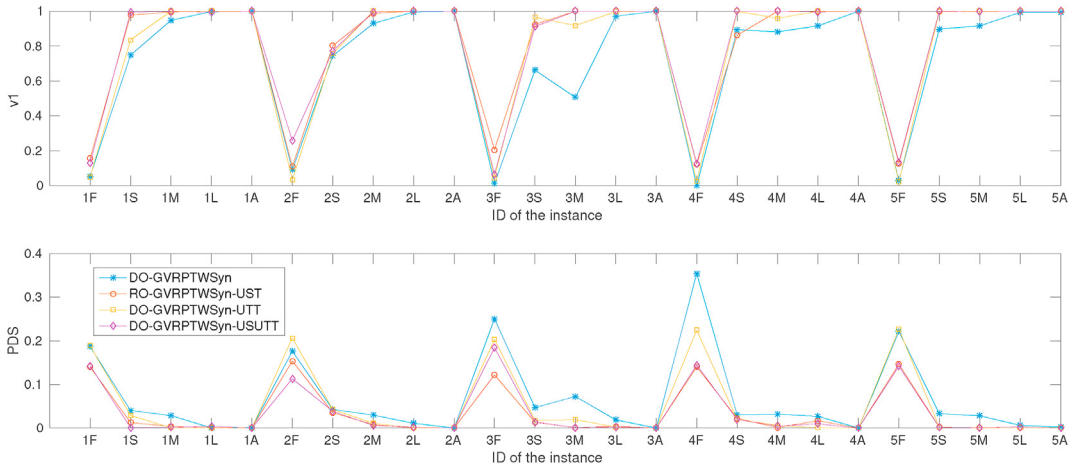

Fig. 13. The indicators of v_1 and PDS for the solutions obtained by four different models.

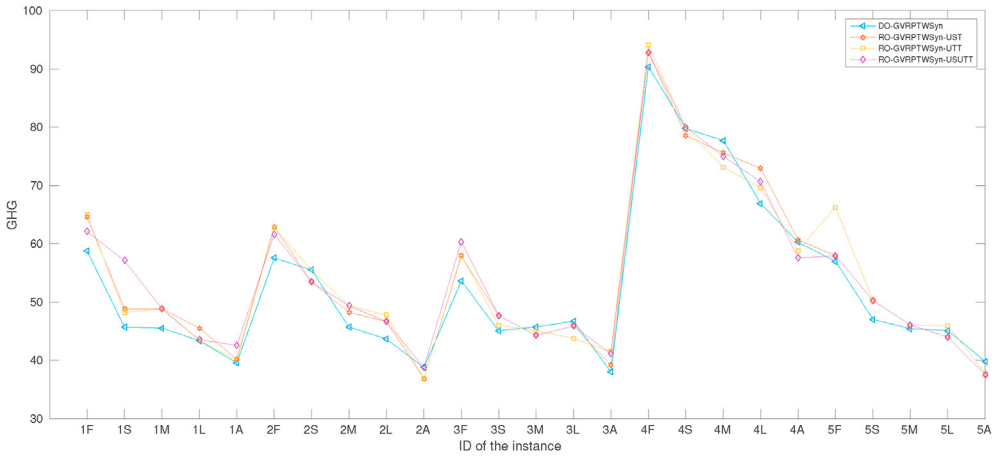

Fig. 14. The values of greenhouse gas emission for the solutions obtained by four different models.

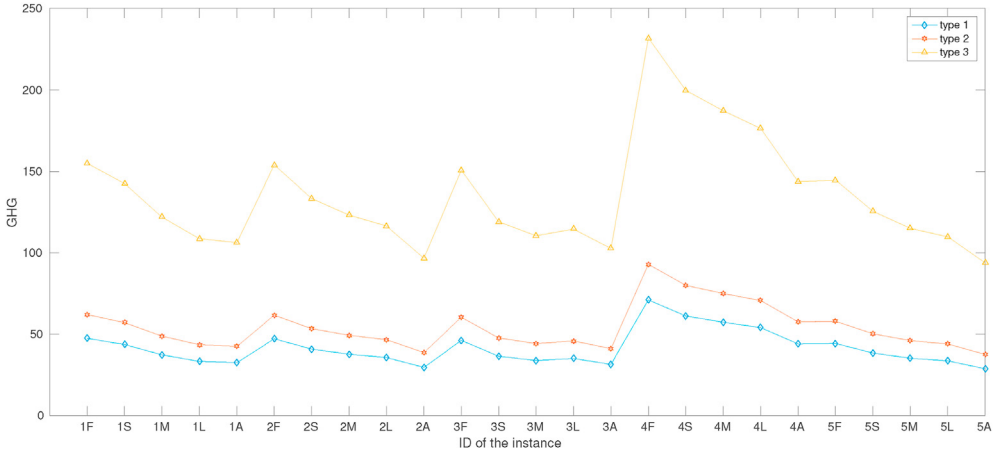

Fig. 15. The change of the amount of fuel consumption cost with the different types of vehicles.

6.1. Introduction to the benchmark instances

As the proposed model in this article is quite novel, there are no existing instances that are entirely consistent with this article. The instances are generated by modifying the widely used benchmark instances, which are initially proposed by Bredström and Rönnqvist (2008).

For each instance, the customers are located in a squared area, while the unique depot is at the center of the current region. There are about 10% of the customers demand simultaneous service from two different workers. Bredström and Rönnqvist (2008) make the first trial to solve these instances by using CPLEX solver and a heuristic algorithm. They found that CPLEX solver cannot obtain the optimal solution for most of these instances in a reasonable time (120 min), and also some near-optimal results were reported in this paper.

Given the feature of different kinds of time windows, the instances of Bredström and Rönnqvist (2008) are classified into five groups, which are displayed in Table 5. As an example, in the last column, E represents the earliest service time, while L indicates the latest service time.

Table 6 presents the critical parameters, which are empirically chosen in the algorithms and models according to the combination of Design of Experiments (DOE) (Fisher, 1936).

6.2. Experimental results on the deterministic model

Because previous studies did not have exactly the same model as this study, therefore, the optimal solutions obtained by this model cannot be directly compared with the previously published research. However, as an essential principle, all heuristic algorithms need to verify the validity before they are approved. This section aims to test the performance of the hybrid SA and TS. First, the model is degenerated into a VRPTWsyn (Bredström and Rönnqvist, 2008; Afifi et al., 2016) and transform the objective function to minimize travel time (converted to hours). Then the designed SA-TS algorithm is implemented to solve the degraded problem directly.

Table 7 reports optimal objective values obtained by the proposed approach, as well as the comparison conducted with the published results.

First of all, it is noticed that all the numbers of used vehicles are exactly the same as the solutions in Bredström and Rönnqvist (2008) and Afifi et al. (2016). When compared with the results reported by Bredström and Rönnqvist (2008), it is found that 11 (44.00%)solutions are tied, and 12 (48.00%) solutions are improved. Therefore, the solutions obtained by the proposed approach show better performance than the heuristic designed by Bredström and Rönnqvist (2008). When compared with one of the fresh publication (Afifi et al., 2016), our results still have ten solutions (66.7%) are equal to the best-known results. There are two improved solutions,

Table 7
The experimental results for the deterministic model.

ID of instance	BKS in Afifi et al. (2016))		Bredström and Rönnqvist (2008)		our proposed approach(SA-TS)			gap1	gap2
	TT (h)	NV	TT (h)	NV	TT(h)	NV	cpu(s)		
1F	- *	- *	5.13	4	5.13	4	2.22	0.00%	- *
1S	3.55	4	3.55	4	3.55	4	1.93	0.00%	0.00%
1M	3.55	4	3.55	4	3.55	4	1.94	0.00%	0.00%
1L	3.39	4	3.44	4	3.39	4	1.94	−1.45%	0.00%
1A	–	–	3.16	4	3.13	4	3.38	−0.95%	–
2F	–	–	4.98	4	4.98	4	1.99	0.00%	–
2S	4.27	4	4.27	4	4.27	4	1.95	0.00%	0.00%
2M	3.58	4	3.58	4	3.58	4	2.28	0.00%	0.00%
2L	3.42	4	3.58	4	3.42	4	2.49	−4.47%	0.00%
2A	–	–	3.58	4	2.97	4	3.72	−17.04%	–
3F	–	–	5.19	4	5.19	4	2.01	0.00%	–
3S	3.63	4	3.63	4	3.53	4	1.88	−2.75%	−2.75%
3M	3.33	4	3.41	4	3.44	4	1.89	0.88%	3.30%
3L	3.29	4	3.29	4	3.29	4	1.98	0.00%	0.00%
3A	–	–	3.1	4	2.91	4	3.18	−6.13%	–
4F	–	–	7.21	4	7.21	4	2.17	0.00%	–
4S	6.14	4	6.14	4	6.12	4	1.97	−0.33%	−0.33%
4M	5.67	4	5.91	4	5.67	4	1.85	−4.06%	0.00%
4L	5.13	4	5.83	4	5.17	4	1.89	−11.32%	0.78%
4A	–	–	5.23	4	4.4	4	2.6	−15.87%	–
5F	–	–	5.37	4	5.37	4	2.19	0.00%	–
5S	3.93	4	3.93	4	3.97	4	2.14	1.02%	1.02%
5M	3.53	4	3.53	4	3.53	4	2.05	0.00%	0.00%
5L	3.34	4	3.43	4	3.34	4	1.97	−2.62%	0.00%
5A	–	–	3.26	4	2.91	4	3.3	−10.74%	–
Average value							2.27	−3.03%	0.13%

BKS: best known solution.
TT: the total travel time.
NV: the number of the used vehicles.
cpu: the computing time.
gap1.$(TT_{\text{our resuts}} - TT_{\text{Bredström and Rönnqvist (2008)}})$*100%/$TT_{\text{Bredström and Rönnqvist (2008)}}$
gap2.$(TT_{\text{our resuts}} - TT_{\text{Afifi et al. (2016)}})$*100%/$TT_{\text{Afifi et al. (2016)}}$
★:Afifi et al. (2016) just reported a part of the solutions, therefore, - is used to indicate the undisclosed solutions.

Table 8
The results of Fridman-test for validating the difference of the four models.

indicator	V0				GHG			
ID of model	DO.	UST.	UTT.	USUTT.	DO.	UST.	UTT.	USUTT.
P-value	9.50×10^{-7}				8.07^{-15}			

DO.: DO-GVRPTWSyn model.
UST.: RO-GVRPTWSyn-UST model.
UTT.: RO-GVRPTWSyn-UTT model.
USUTT.: RO-GVRPTWSyn-USUTT model.

while only three solutions are worse than the given best know solutions.

It should be emphasized that the main purpose of our research is not to propose a novel algorithm for obtaining the better solutions than the published results, but here is for validating the efficiency and effectiveness of the proposed heuristic algorithm.

According to the aforementioned analysis, our experimental results demonstrate that the proposed hybrid SA-TS can effectively solve the benchmark instances of Bredström and Rönnqvist (2008). Additionally, considering that the computing time is short (around 2 s), it is found that the proposed hybrid SA-TS is efficiency. The next sections will show the experimental results on the robust optimization models.

6.3. Experimental results on the robust optimization models

After validating the proposed heuristic, SA-TS is applied to solve the RO model. As pointed out, our work involves four kinds of scenarios/models. The scenarios can be listed as follows.

(1) DO-GVRPTWSyn: The deterministic optimization model without considering any uncertainties.
(2) RO-GVRPTWSyn-UST: The robust optimization model with considering only the uncertain service time of customers.
(3) RO-GVRPTWSyn-UTT: The robust optimization model with considering only travel time on the driving duration.
(4) RO-GVRPTWSyn-USUTT: The robust optimization model with taking into account both client's service time and worker's travel time simultaneously.

Now it is time to consider the two core issues of this article. The first question is: how to measure the robustness performance of the solutions obtained by the four models? The second question is: what are the differences among the greenhouse gas emissions obtained in these four scenarios?

To answer these two questions, first of all, some observing indicators are defined to describe the robustness performance, then the Monte Carlo simulation (see Fig. 4) is employed to simulate each indicator.

The indicators can be viewed as a mapping from a feasible solution to real numbers, which can be expressed as follows.

The basic mathematical principles of Monte Carlo simulation are derived from the Law of Large Numbers in probability theory & mathematical statistics. For a given instance, four optimal solutions could be obtained from the four models. For these four solutions, it is assumed that they are in an uncertain environment, which simulates uncertain practical scenarios. Finally, the indicators of robustness and greenhouse gas emissions are obtained through

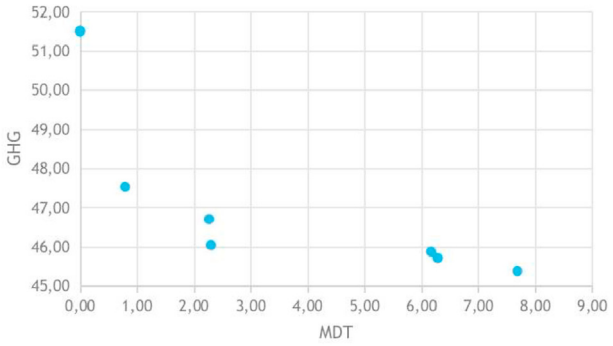

Fig. 16. Pareto frontier of scenario I.

Monte Carlo simulation. The difference in the model is inferred by comparing the differences between the indicators.

6.3.1. The impact of time windows

As introduced, the instances featured with different types of time windows are divided into different groups. This section mainly investigated how the length of the time windows affect the robustness and greenhouse gas emissions indicators.

Firstly, the optimal solutions from the RO-GVRPTWSyn-USUTT for all instances are obtained. The Monte Carlo simulation is performed on these solutions to output the indicators, which are shown in Fig. 5. Each indicator represents the average values of the same type of time window. Therefore, the simulation results of five groups, namely F, S, M, L and A, are obtained and compared.

As shown in Fig. 5 (a), the instances with fixed time windows have very low values in v_0, which means the robustness performance is very poor. On the contrary, the categories of M, L are very high; What's more, it is found that this value for A group is almost equal to one, which reveals a feature of strong robustness. The similar situation is also shown in Fig. 5 (b).

On the other side of the indicators, such as mean delayed time in Fig. 5 (c), it is found that the group of F and S have a very high delayed time for providing service, while the groups named M, L, and A becomes small values. Notably, the group with A has almost zero means of delayed time.

When analyzing the fuel consumption cost in Fig. 5 (d), it is noticed that the values, from left to right, show a trend of severe decline.

To sum up, it is found that the robustness becomes stronger when the time windows become large, while for those instances with a small or fixed time window, it's challenging to improve the solutions to realize the complete robustness.

6.3.2. Scenario 1: only uncertain travel time is considered

In this scenario, a robust model called RO-GVRPTWSyn-UTT is considered. In this scenario, it is only assumed that travel time is uncertain while the service time is deterministic. This comparison helps us to validate if the components of considering the travel time uncertainty can really increase the robustness of the obtained solution.

In RO-GVRPTWSyn-UTT, the LPAT for each customer is calculated according to the formulation (22). The experiments are performed in the following way.

(1) Obtain the solution of each instance corresponding to the deterministic model DO-GVRPTWSyn.
(2) Obtain the solutions of RO-GVRPTWSyn-UTT for each instance.
(3) Assume that these solutions are in an uncertain environment, then the Monte Carlo simulation is applied to each solution and output the indicators.

The simulating indicators of the solutions are presented in Figs. 6 and 7 it is noticed that in Fig. 6, a blue line with diamonds is always above the red line with rectangles. For example, let us focus on the v_0. For the instance 1M, the value of v_0 is around 50%, while this value becomes 99%. This means that there are 50% of the simulation times, in which non customer is received delayed service in DO-GVRPTWSyn, while in RO-GVRPTWSyn-UTT, this value increase to 99%, which illustrates a strong robustness. In Fig. 7, it is found that the blue line with diamonds somehow shows smaller than the red line with rectangles. Let us focus on the first subplot of Fig. 7, which illustrates the percentage of the delayed service (PDS). For the instance 4M, in DO-GVRPTWSyn, the value of PDS is around 4%, while this value becomes less than 1% in the RO-GVRPTWSyn-UTT. This also indicates that the percentage of the delayed service can be decreased by the RO-GVRPTWSyn-UTT model.

The comparisons in this section reveal that the robustness is enhanced when considering the uncertain travel time.

6.3.3. Scenario 2: only uncertain service time is considered

In this scenario, a robust model called RO-GVRPTWSyn-UST is considered. In the scenario, it is only assumed that service time is uncertain while the travel time is deterministic. This comparison helps us to validate if the components of considering the service time uncertainty can really increase the robustness of the obtained solution.

In RO-GVRPTWSyn-UST, the largest arrival time for each customer is calculated according to the formulation (21). The experiments are performed in the following way.

(1) Obtain the solution of each instance corresponding to the deterministic model DO-GVRPTWSyn.
(2) Obtain the solutions of RO-GVRPTWSyn-UST for each instance.
(3) Assume that these solutions are in an uncertain environment, then the Monte Carlo simulation is applied to each solution and output the indicators.

The simulating indicators of the solutions are presented in Figs. 8 and 9. It is noticed that in Fig. 6, a blue line with diamonds is always above the red line with rectangles. For example, the indicator v_0, for the instance 1M, the value of v_0 is around 50%, while this value increases to 97%. This means that there are 50% of the simulation times that non-customer is received delayed service in DO-GVRPTWSyn, while in RO-GVRPTWSyn-UST, 97% of the simulation times with the situation that non-customers have received delayed service. In Fig. 9, it is found that the blue line with diamonds somehow shows smaller than the red line with rectangles. For example. in Fig. 9, it is found that the percentage of the delayed service for the instance 4M in DO-GVRPTWSyn, is around 4%, while this value becomes less than 1% when solved by RO-GVRPTWSyn-UST. These comparisons reveal that the robustness is enhanced when considering the uncertain travel time.

Additionally, in Fig. 9, it is noticed that the indicators for delayed service for RO-GVRPTWSyn-UST model are always smaller than that of DO-GVRPTWSyn model. This reveals that the RO-GVRPTWSyn-UST model can help the logistics company to reduce the delayed service.

6.3.4. Scenario 3: UTT and UST are considered simultaneously

In scenarios 1 and 2, each component of the uncertainties has been validated to improve the robustness performance. In this

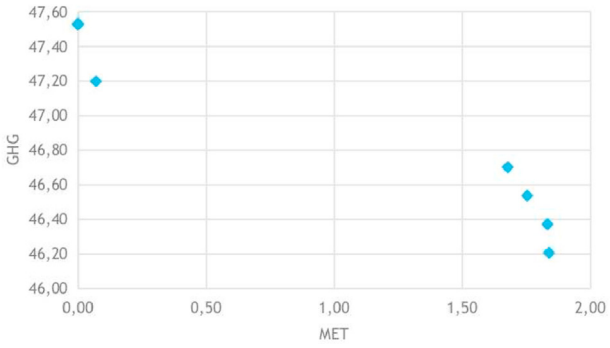

Fig. 17. Pareto frontier of scenario II.

section, the RO-GVRPTWSyn-USUTT model, a more comprehensive consideration of UST and UTT, is analyzed. To highlight the importance of considering the uncertainties, the different solutions for the same instance but obtained by the DO-GVRPTWSyn and the RO-GVRPTWSyn-USUTT are compared.

The simulation results are presented in Figs. 10 and 11. It is noticed that in Fig. 10, a blue line with diamonds is always above the red line with rectangles. For example, it is found the v_1, for the instance 3M is around 50%, while this value becomes 100%. This means that there are 50% of the simulation times have at most one customer is received delayed service in DO-GVRPTWSyn, while in RO-GVRPTWSyn-USUTT, this value becomes 100%, which reveals that 100% times of the simulation showed at most one delayed service. In Fig. 11, it is found that the blue line with diamonds somehow shows smaller than the red line with rectangles. For example in Fig. 11, let us focus on the percentage of the delayed service (PDS). For instance 4M, in DO-GVRPTWSyn, the value of PDS is around 4%, while this value decreases to 0%, which means no delayed service.

Fig. 12 reports the simulation results for the solutions obtained by the DO-GVRPTWSyn and RO-GVRPTWSyn-USUTT for v_3 and fuel consumption cost with the large size instances. From the observation of v_3, it is found that most of the solutions obtained by RO-GVRPTWSyn-USUTT are shown much higher than those solutions produced by the DO-GVRPTWSyn model. For example, it is noticed that, in the instance 9M, the value of v_3 is tiny in the DO-GVRPTWSyn model, while it reaches close to 1 (high robustness) when applying RO-GVRPTWSyn-USUTT model. Additionally, it is found that in most instances, the fuel consumption cost increases a little when utilizing the RO-GVRPTWSyn-USUTT model. This reveals a trade-off relationship between the robustness and fuel consumption cost.

6.4. Comparison among the four models

In the previous sections, verification of the robustness considerations for each component has been checked. This section mainly analyzes the different robustness performances for the solutions obtained from these different scene models. According to the previous method, a comparative analysis is conducted. Due to the limited space, the selected representative indicators, v_1 and PDS, are shown in Fig. 13. It is found that robustness performance could be improved if UST and UTT are taken into account. While the scheduling obtained without considering any uncertainties shows poor robustness performance. If only one kind of uncertainty, either UTT or UST, is considered, although the robustness is not as good as the solution obtained by the model considering both, it is still much stronger than without considering any uncertainties. Therefore, considering uncertainty is essential and can effectively improve operational efficiency.

As shown in Fig. 14, it is found that the different values of the greenhouse gas emission in different four models for each instance. It is noticed that the solutions obtained by the DO-GVRPTWSyn model generate a smaller amount of greenhouse gas emissions than others. This illustrates the trade-off relationship between the robustness and the amount of greenhouse gas emissions. However, it is found that the robustness can be significantly improved only by a little improvement in the greenhouse gas emission.

6.5. Sensitivity analysis of the uncertain parameters

As mentioned before, the type of employed vehicles may also affect fuel consumption costs. Now, it is time to analyze how the type of vehicle affects greenhouse gas emissions. As seen in Fig. 15, it found that the fuel consumption cost with type 3 vehicles is strictly higher than the other two types. For example, if vehicles are changed from type 2 to type 1, the solution can decrease the fuel consumption cost, while it will have a steeply increase if the type of vehicles is switched to type 3.

6.6. Statistical analysis

In order to further quantitatively compare the differences among the proposed four models, the Friedman-test is performed to test independent experimental samples. If someone is interested in this method, please refer to the literature (Birch, 1983). Three indicators (which can also be extended to all indicators) are selected and tested whether the three indicators performed differently in the four models. The results are shown in Table 8.

As a classical paradigm in the statistic test, the hypothesis is presented with H_0 and H_1. The H_1 holds when H_0 is rejected; otherwise, H_0 holds. In our work, the H_0 and H_1 are displayed as follows.

H_0: The solutions achieved by the four models have no significant difference in terms of the observing indicators.
H_1: The solutions achieved by the four models have significant differences, given the observing indicators.

As displayed in Table 8, the p-value for each model is reported. When comparing the four models for the indicator V_0, it is indicated that the p-value is 9.50×10^{-7}, which is less than the threshold of 0.5% (reject H_0). This indicates that the four models are quite different in terms of the solutions. Besides, it is found that the p-value for indicators of GHG emission is 8.07^{-15}, which also rejects the H_0. It is surely confirmed that there are significant differences between the solutions achieved by the four models. According to the ranking discussed in section 6.4, the conclusion could be reached that the RO models show better robustness performance than the deterministic model. Also, from this test, it is validated that the different changes in GHG emissions for the solutions achieved by the different scenarios.

6.7. Experimental results for the Pareto-based bi-objective optimization scenarios

The numerical results obtained by the mono-objective model

have been intensively discussed in different scenarios. Although the mono-objective models have been commonly investigated in the VRPs with uncertain optimization, they still have limitations in exploring the conflicts between the different objective functions. The purpose of this section is to establish a multi-objective optimization framework based on the presented model and analyze the trade-off relationship between the GHG emission and other robustness indicators. According to our problem's feature, two objectives are considered; therefore, our model can also be called bi-objective optimization (Fathollahi-Fard et al., 2020).

The bi-objective optimization is based on the concept of Pareto optimization, which is defined as follows.

Definition 6.1. The bi-objective optimization problem is defined as follows.

$$\begin{aligned} &\min_{x\in X} f(x) = [f_1(x), f_2(x)]^T \\ &X \subseteq R^m \end{aligned} \tag{26}$$

Where $f_1(\cdot)$ and $f_2(\cdot)$ are the objective functions of problem. X is the set of the feasible solutions and x is one of the feasible solutions. It is assumed that x_1 and x_2 are the two solutions of the optimization problem, then three relationships between x_1 and x_2 are defined as follows.

(1) x_1 dominates x_2, when $f_1(x_1) < f_1(x_2)$ and $f_2(x_1) <= f_2(x_2)$, or $f_1(x_1) <= f_1(x_2)$ and $f_2(x_1) < f_2(x_2)$.
(2) x_2 dominates x_1, when $f_1(x_1) > f_1(x_2)$ and $f_2(x_1) >= f_2(x_2)$, or $f_1(x_1) >= f_1(x_2)$ and $f_2(x_1) > f_2(x_2)$.
(3) x_2 and x_1 cannot be dominated each other, otherwise.

Two scenarios, namely *scenario I* and *scenario II* are defined according to the model. GHG emission is selected as one objective function since it is the main issue in the article. MDT or MET is selected as another indicator in the bi-objective optimization model since ADT and MET are typical robustness indicators from different decision-makers' perspectives. ADT measures the degree of delayed services, while MET, namely the mean extra working time of workers, indicates the welfare of workers.

Scenario I aims at minimizing the GHG emissions and mean delayed time simultaneously. The scenario is formulated as equation (27).

$$\begin{cases} \min f_1 = \sum_{k\in V}\sum_{j\in N}\sum_{i\in N} FuelCost_{ijk}(s,t), \\ \min f_2 = MDT(s,t), \end{cases} \tag{27}$$

Constraints (5)–(9) and (23).where, the first objective function is the GHG emission function while the second objective function is the mean delayed time function defined in Fig. 4. The meaning of the other parts of the formulation is show in objective function (17).

scenario II aims at minimizing the GHG emissions and mean extra working time for delivery workers simultaneously. The scenario is formulated as equation (28).

$$\begin{cases} \min f_1 = \sum_{k\in V}\sum_{j\in N}\sum_{i\in N} FuelCost_{ijk}(s,t), \\ \min f_2 = MET(s,t), \end{cases} \tag{28}$$

Constraints (5)–(9) and (23).where, the first objective function is the GHG emission function while the second objective function is the mean extra working time for delivery workers which is defined in Fig. 4. The meaning of the other parts of the formulation is show in objective function (17).

6.7.1. The pseudo of the algorithm

At present, a variety of multi-objective simulated annealing (MOSA) algorithms have been investigated. One of the most commonly used algorithms is called SMOSA, which was proposed by Suppapitnarm et al. (2000). Therefore, in this work, the bi-objective optimization models, namely scenario I and scenario II, are also solved by the Pareto-based SA-TS, which is abbreviated as SMOSATS. The basic procedures of SMOSATS are presented in Algorithm 4.

Algorithm 4. SMOSATS.

step 1. Initialize the temperature T as T_0 and total iterations $maxgen$. Set the terminal criteria: either the $T < \epsilon$ or the current generation reaches $maxgen$.
step 2. Generate the initial solution x_0 by using the algorithm 1 and algorithm 2. Calculate all its objective function values and add them to the Pareto solution set. Set x_0 the current solution $x_{current}$.
step 3. Apply the tabu search to $x_{current}$, then generate the neighborhood solution x_{new}, and calculate objective function values of x_{new}.
step 4. Compare the newly generated solution x_{new} with each solution in the Pareto solution set and update the Pareto solution set.
step 5. If the new neighborhood solution x_{new} enters the Pareto solution set, Replace x_{new} with $x_{current}$ and go to step 8.
step 6. Calculate the acceptance probability with the formulation (29).
step 7. If x_{new} does not enter the Pareto solution set, then decide whether to accept the new solution according to the acceptance probability with formulation (29). If the new solution is accepted, let it be the new current solution $x_{current}$, if x_{new} is not accepted, keep the current solution.
step 8. At a certain number of iterations $\hat{N}$, randomly select a solution from the Pareto solution set it as the $x_{current}$ and search again.
step 9. Perform a cooling stage with the formulation: $T \leftarrow \zeta * T$.
step 10. Repeat Step 3 to Step 9 until the algorithm reaches the terminal criteria.
Output: the best Pareto frontier.

The criteria for accepting a new solution is one of the features of the MOSA-TS. Suppapitnarm et al. (2000) designed the SMOSA algorithm and used a return value-based strategy to start searching from the archived solutions in the solution space.

The main difference between multi-objective SA and single-objective SA lies in the way how a new solution is accepted. In mono-objective optimization, when the new solution is better than the current solution, the newly generated solution is 100% accepted. When the newly generated solution is worse than the current solution, this new solution is accepted in a function $exp(\cdot)$ of probability (the idea of simulated annealing). In the multi-objective problem, the dominance of different solutions is considered. When the solution is superior or non-dominant, the new solution is directly accepted and archived it in the optimal frontier. When the solution is worse than the current solution, the following probability function (29) is used to receive the solution.

$$p = \min\left(1, \prod_{i=1}^{2} \exp\left\{\frac{f_i(x_{current}) - f_i(x_{new})}{T_i}\right\}\right) \tag{29}$$

6.7.2. The experimental results

In this section, the experimental results for the multi-objective optimization are presented. It should be emphasized that our paper's purpose is not to make a decision for the logistics companies directly. But, the framework is established to provide the decision-support solutions to the logistics companies, so that the decision-makers could select the strategy according to their preference. An example with the instance 1M is given as follows, and the parameter for the algorithm is the same as Table 7.

The Pareto frontiers, composed by the objective values of the best non-dominated solutions, show in Figs. 16 and 17. As shown in Fig. 16, it is found that as MDT increases, GHG decreases. This demonstrates that the MDT and GHG shows a trade-off relationship. In Fig. 17, it is found that the similar trend as Fig. 16. However, when compared with the two Pareto frontiers, it is indicated that GHG's change has a big impact on the MDT, while it has less impact on MET.

The proposed bi-objective optimization framework and the Pareto frontiers obtained in different scenarios could help the logistics companies make a reasonable decision when planning logistics activities.

7. Conclusions

Nowadays, logistics companies need not only consider improving service quality and reducing operating costs but also should take a certain corporate social responsibility: reducing greenhouse gas emissions. This study investigated a relative robust optimization model for a VRPTW with synchronized visits and uncertain scenarios considering greenhouse gas emissions. Considering the problem is NP-hard, a hybrid algorithm is developed to solve the optimization model. The experimental results illustrate the following conclusions.

(1) The experimental results on the popularly used benchmark instances demonstrates that the proposed hybrid SA-TS algorithm has a good performance.
(2) The comparison performed among the solutions obtained by different models has highlighted the importance of considering uncertainties.
(3) The sensitivity analysis of greenhouse gas emissions with different types of vehicles shows the difference of the GHG emission in different vehicle types. This gives the decision-maker a choice to select the type of vehicle when arranging the routes.
(4) Pareto-based the bi-objective optimization with two scenarios validates the trade-off between the robustness indicators and GHG emissions.

The proposed model has the potential to be applied to some practical applications, such as logging truck routing planning. This research has many interesting extensions worthy of being investigated. On the one hand, some new ideas, for example, learning-based strategy and multi-agent systems, can be incorporated to guide hybrid SA-TS to improve the solution quality further. On the other hand, some emerging technologies, such as drones, will be considered in logistics planning, thereby improving logistics operation efficiency and reducing labor costs.

Declaration of competing interest

The authors declare that they have no known competing financial interests or personal relationships that could have appeared to influence the work reported in this paper.

Acknowledgments

We thank the anonymous reviewers and editors for their valuable comments, which helped us improve the paper a lot. We acknowledge Prof. Bredström and Rönnqvist (2008) for kindly providing us the benchmark instances. The first author gratefully thanks the precious funding supported by European Union's Horizon 2020 research program (Grant Agreement No. 727520), French National Research Agency (Grant Agreement No. ANR-16-CONV-0003), and China Scholarship Council (contract Nos. 201504490047 and 201608260014).

References

Abdi, A., Abdi, A., Akbarpour, N., Amiri, A.S., Hajiaghaei-Keshteli, M., 2019. Innovative approaches to design and address green supply chain network with simultaneous pick-up and split delivery. J. Clean. Prod., 119437 https://doi.org/10.1016/j.jclepro.2019.119437.

Afifi, S., Dang, D.C., Moukrim, A., 2016. Heuristic solutions for the vehicle routing problem with time windows and synchronized visits. Optimization Letters 10, 511–525.

Agra, A., Christiansen, M., Figueiredo, R., Hvattum, L.M., Poss, M., Requejo, C., 2013. The robust vehicle routing problem with time windows. Comput. Oper. Res. 40, 856–866.

Almouhanna, A., Quintero-Araujo, C.L., Panadero, J., Juan, A.A., Khosravi, B., Ouelhadj, D., 2020. The location routing problem using electric vehicles with constrained distance. Comput. Oper. Res. 115, 104864.

Alvarez, A., Munari, P., 2017. An exact hybrid method for the vehicle routing problem with time windows and multiple deliverymen. Comput. Oper. Res. 83, 1–12.

Anderluh, A., Larsen, R., Hemmelmayr, V.C., Nolz, P.C., 2019a. Impact of travel time uncertainties on the solution cost of a two-echelon vehicle routing problem with synchronization. Flex. Serv. Manuf. J. 1–23.

Anderluh, A., Nolz, P.C., Hemmelmayr, V.C., Crainic, T.G., 2019b. Multi-objective optimization of a two-echelon vehicle routing problem with vehicle synchronization and 'grey zone' customers arising in urban logistics. Eur. J. Oper. Res. https://doi.org/10.1016/j.ejor.2019.07.049.

Bahadori-Chinibelagh, S., Fathollahi-Fard, A.M., Hajiaghaei-Keshteli, M., 2019. Two constructive algorithms to address a multi-depot home healthcare routing problem. IETE J. Res. 1–7.

Basso, R., Kulcsár, B., Egardt, B., Lindroth, P., Sanchez-Diaz, I., 2019. Energy consumption estimation integrated into the electric vehicle routing problem. Transport. Res. Transport Environ. 69, 141–167.

Bektaş, T., Laporte, G., 2011. The pollution-routing problem. Transp. Res. Part B

Methodol. 45, 1232–1250.
Ben-Tal, A., Nemirovski, A., 1999. Robust solutions of uncertain linear programs. Oper. Res. Lett. 25, 1–13.
Birch, D., 1983. Statistical Rank and the Friedman Test as an Indication of Significance in the Preliminary Stages of a Multi-Variable Analysis of Literary Texts.
Bredström, D., Rönnqvist, M., 2008. Combined vehicle routing and scheduling with temporal precedence and synchronization constraints. Eur. J. Oper. Res. 191, 19–31.
Cappanera, P., Scutellŕ, M.G., Nervi, F., Galli, L., 2018. Demand uncertainty in robust home care optimization. Omega 80, 95–110.
Chu, X., Xu, S.X., Cai, F., Chen, J., Qin, Q., 2019. An efficient auction mechanism for regional logistics synchronization. J. Intell. Manuf. 30, 2715–2731.
Decerle, J., Grunder, O., El Hassani, A.H., Barakat, O., 2018. A memetic algorithm for a home health care routing and scheduling problem. Operations research for health care 16, 59–71.
Decerle, J., Grunder, O., El Hassani, A.H., Barakat, O., 2019. A memetic algorithm for multi-objective optimization of the home health care problem. Swarm and evolutionary computation 44, 712–727.
Ding, T., Wu, H., Jia, J., Wei, Y., Liang, L., 2020. Regional assessment of water-energy nexus in China's industrial sector: an interactive meta-frontier dea approach. J. Clean. Prod. 244, 118797.
Drexl, M., 2012. Synchronization in vehicle routin––a survey of vrps with multiple synchronization constraints. Transport. Sci. 46, 297–316.
Elhedhli, S., Merrick, R., 2012. Green supply chain network design to reduce carbon emissions. Transport. Res. Transport Environ. 17, 370–379.
En-nahli, L., Afifi, S., Allaoui, H., Nouaouri, I., 2016. Local search analysis for a vehicle routing problem with synchronization and time windows constraints in home health care services. IFAC-PapersOnLine 49, 1210–1215.
Faiz, T.I., Vogiatzis, C., Noor-E-Alam, M., 2019. A column generation algorithm for vehicle scheduling and routing problems. Comput. Ind. Eng. 130, 222–236.
Fathollahi-Fard, A.M., Ahmadi, A., Goodarzian, F., Cheikhrouhou, N., 2020. A bi-objective home healthcare routing and scheduling problem considering patients' satisfaction in a fuzzy environment. Appl. Soft Comput. 106385.
Fathollahi-Fard, A.M., Govindan, K., Hajiaghaei-Keshteli, M., Ahmadi, A., 2019. A green home health care supply chain: new modified simulated annealing algorithms. J. Clean. Prod. https://doi.org/10.1016/j.jclepro.2019.119437.
Fathollahi-Fard, A.M., Hajiaghaei-Keshteli, M., Tavakkoli-Moghaddam, R., 2018. A bi-objective green home health care routing problem. J. Clean. Prod. 200, 423–443.
Fisher, R.A., 1936. Design of experiments. Br. Med. J. 1, 554–554.
Frifita, S., Masmoudi, M., 2020. Vns methods for home care routing and scheduling problem with temporal dependencies, and multiple structures and specialties. Int. Trans. Oper. Res. 27, 291–313.
Fu, Y., Tian, G., Fathollahi-Fard, A.M., Ahmadi, A., Zhang, C., 2019. Stochastic multi-objective modelling and optimization of an energy-conscious distributed permutation flow shop scheduling problem with the total tardiness constraint. J. Clean. Prod. 226, 515–525.
Ganji, M., Kazemipoor, H., Molana, S.M.H., Sajadi, S.M., 2020. A green multi-objective integrated scheduling of production and distribution with heterogeneous fleet vehicle routing and time windows. J. Clean. Prod. 120824.
Giallanza, A., Puma, G.L., 2020. Fuzzy green vehicle routing problem for designing a three echelons supply chain. J. Clean. Prod. 120774.
Glover, F., 1989. Tabu search––part i. ORSA J. Comput. 1, 190–206.
Glover, F., 1990. Tabu search––part ii. ORSA J. Comput. 2, 4–32.
Grenouilleau, F., Legrain, A., Lahrichi, N., Rousseau, L.M., 2019. A set partitioning heuristic for the home health care routing and scheduling problem. Eur. J. Oper. Res. 275, 295–303.
Haddadene, A., Roufaida, S., Labadie, N., Prodhon, C., 2019. Bicriteria vehicle routing problem with preferences and timing constraints in home health care services. Algorithms 12, 152.
Haddadene, S.R.A., Labadie, N., Prodhon, C., 2016. A grasp× ils for the vehicle routing problem with time windows, synchronization and precedence constraints. Expert Syst. Appl. 66, 274–294.
He, Z., Chen, P., Liu, H., Guo, Z., 2017. Performance measurement system and strategies for developing low-carbon logistics: a case study in China. J. Clean. Prod. 156, 395–405.
Hockstad, L., Hanel, L., . reportInventory of U.S. Greenhouse Gas Emissions and Sinks. Technical Report. doi:10.15485/1464240.
Hojabri, H., Gendreau, M., Potvin, J.Y., Rousseau, L.M., 2018. Large neighborhood search with constraint programming for a vehicle routing problem with synchronization constraints. Comput. Oper. Res. 92, 87–97.
Hossein, H.D., Gilles, P., Louis-Martin, R., 2019. Vehicle routing problems with synchronized visits and stochastic travel and service times: applications in healthcare. Transport. Sci. https://doi.org/10.1287/trsc.2019.0956.
Hu, C., Lu, J., Liu, X., Zhang, G., 2018. Robust vehicle routing problem with hard time windows under demand and travel time uncertainty. Comput. Oper. Res. 94, 139–153.
Hu, Z.H., Wei, C., 2018. Synchronizing vehicles for multi-vehicle and one-cargo transportation. Comput. Ind. Eng. 119, 36–49.
Kara, I., Kara, B.Y., Yetis, M.K., 2007. Energy minimizing vehicle routing problem. In: International Conference on Combinatorial Optimization and Applications. Springer, pp. 62–71.
Kirkpatrick, S., Gelatt, C.D., Vecchi, M.P., 1983. Optimization by simulated annealing. Science 220, 671–680.
Kolen, A.W., Rinnooy Kan, A., Trienekens, H.W., 1987. Vehicle routing with time windows. Oper. Res. 35, 266–273.
Li, H., Wang, H., Chen, J., Bai, M., 2020a. Two-echelon vehicle routing problem with satellite bi-synchronization. Eur. J. Oper. Res. https://doi.org/10.1016/j.ejor.2020.06.019.
Li, J., Qin, H., Baldacci, R., Zhu, W., 2020b. Branch-and-price-and-cut for the synchronized vehicle routing problem with split delivery, proportional service time and multiple time windows. Transport. Res. E Logist. Transport. Rev. 140, 101955.
Li, J.q., Han, Y.q., Duan, P.y., Han, Y.y., Niu, B., Li, C.d., Zheng, Z.x., Liu, Y.p., 2020c. Meta-heuristic algorithm for solving vehicle routing problems with time windows and synchronized visit constraints in prefabricated systems. J. Clean. Prod. 250, 119464.
Li, Y., Soleimani, H., Zohal, M., 2019. An improved ant colony optimization algorithm for the multi-depot green vehicle routing problem with multiple objectives. J. Clean. Prod. 227, 1161–1172.
Lin, C.C., Hung, L.P., Liu, W.Y., Tsai, M.C., 2018. Jointly rostering, routing, and rerostering for home health care services: a harmony search approach with genetic, saturation, inheritance, and immigrant schemes. Comput. Ind. Eng. 115, 151–166.
Liu, B., Zhao, R., 1998. Stochastic Programming and Fuzzy Programming. Tsinghua University Press.
Liu, R., Tao, Y., Xie, X., 2019. An adaptive large neighborhood search heuristic for the vehicle routing problem with time windows and synchronized visits. Comput. Oper. Res. 101, 250–262.
Macrina, G., Pugliese, L.D.P., Guerriero, F., Laporte, G., 2019. The green mixed fleet vehicle routing problem with partial battery recharging and time windows. Comput. Oper. Res. 101, 183–199.
Masmoudi, M.A., Hosny, M., Demir, E., Cheikhrouhou, N., 2018. A study on the heterogeneous fleet of alternative fuel vehicles: reducing co2 emissions by means of biodiesel fuel. Transport. Res. Transport Environ. 63, 137–155.
Montoya, A., Guéret, C., Mendoza, J.E., Villegas, J.G., 2017. The electric vehicle routing problem with nonlinear charging function. Transp. Res. Part B Methodol. 103, 87–110.
Munari, P., Morabito, R., 2018. A branch-price-and-cut algorithm for the vehicle routing problem with time windows and multiple deliverymen. Top 26, 437–464.
Naji, W., Masmoudi, M., Mellouli, R., 2017. A robust-milp for synchronized-mtsptw: application to home health care under uncertainties. In: 2017 4th International Conference on Control, Decision and Information Technologies (CoDIT). IEEE, pp. 1089–1094.
Peker, I., Caybasi, G., Buyukozkan, G., Gocer, F., 2019. Evaluation of home health care vehicle routing methods by intuitionistic fuzzy ahp. In: International Conference on Intelligent and Fuzzy Systems. Springer, pp. 607–615.
Poonthalir, G., Nadarajan, R., Kumar, M.S., 2020. Hierarchical optimization of green routing for mobile advertisement vehicle. J. Clean. Prod. 258, 120661.
Quttineh, N.H., Larsson, T., Lundberg, K., Holmberg, K., 2013. Military aircraft mission planning: a generalized vehicle routing model with synchronization and precedence. EURO Journal on Transportation and Logistics 2, 109–127.
Rodriguez, C., Garaix, T., Xie, X., Augusto, V., 2015. Staff dimensioning in homecare services with uncertain demands. Int. J. Prod. Res. 53, 7396–7410.
Ropke, S., Pisinger, D., 2006. An adaptive large neighborhood search heuristic for the pickup and delivery problem with time windows. Transport. Sci. 40, 455–472.
Shao, S., Xu, G., Li, M., Huang, G.Q., 2019. Synchronizing e-commerce city logistics with sliding time windows. Transport. Res. E Logist. Transport. Rev. 123, 17–28.
Shi, Y., Boudouh, T., Grunder, O., 2017. A hybrid genetic algorithm for a home health care routing problem with time window and fuzzy demand. Expert Syst. Appl. 72, 160–176.
Shi, Y., Boudouh, T., Grunder, O., 2019. A robust optimization for a home health care routing and scheduling problem with consideration of uncertain travel and service times. Transport. Res. E Logist. Transport. Rev. 128, 52–95.
Shi, Y., Boudouh, T., Grunder, O., Wang, D., 2018b. Modeling and solving simultaneous delivery and pick-up problem with stochastic travel and service times in home health care. Expert Syst. Appl. 102, 218–233.
Shi, Y., Zhou, Y., Boudouh, T., Grunder, O., 2020. A lexicographic-based two-stage algorithm for vehicle routing problem with simultaneous pickup–delivery and time window. Eng. Appl. Artif. Intell. 95, 103901. https://doi.org/10.1016/j.engappai.2020.103901.
Solomon, M.M., 1987. Algorithms for the vehicle routing and scheduling problems with time window constraints. Oper. Res. 35, 254–265.
Suppapitnarm, A., Seffen, K.A., Parks, G.T., Clarkson, P., 2000. A simulated annealing algorithm for multiobjective optimization. Eng. Optim. 33, 59–85.
Trautsamwieser, A., Gronalt, M., Hirsch, P., 2011. Securing home health care in times of natural disasters. Spectrum 33, 787–813.
UCS, 2019. Each country's share of CO2 emissions. https://www.ucsusa.org/global-warming/science-and-impacts/science/each-countrys-share-of-co2.html. (Accessed 26 August 2019).

Westcott, B., Wilkinson, D., 2019. UK plans to become first G7 economy with net zero carbon emissions by 2050. https://edition.cnn.com/2019/06/11/uk/uk-carbon-emissions-g7-intl-hnk/index.html. (Accessed 26 August 2019).
Wu, L., Hifi, M., Bederina, H., 2017. A new robust criterion for the vehicle routing problem with uncertain travel time. Comput. Ind. Eng. 112, 607–615.
Xiao, L., Dridi, M., Hajjam El Hassani, A., Fei, H., Lin, W., 2018. An improved cuckoo search for a patient transportation problem with consideration of reducing transport emissions. Sustainability 10, 793.
Xu, S.X., Shao, S., Qu, T., Chen, J., Huang, G.Q., 2018. Auction-based city logistics synchronization. IISE Transactions 50, 837–851.
Zhang, Z., Luo, Z., Qin, H., Lim, A., 2019. Exact algorithms for the vehicle routing problem with time windows and combinatorial auction. Transport. Sci. 53, 427–441.
Zulvia, F.E., Kuo, R., Nugroho, D.Y., 2020. A many-objective gradient evolution algorithm for solving a green vehicle routing problem with time windows and time dependency for perishable products. J. Clean. Prod. 242, 118428.